

RD-A178 255

QUANTITATIVE DETERMINATION OF ENGINE WATER INGESTION
(U) JET PROPULSION LAB PASADENA CA P PARIKH ET AL.

1/1

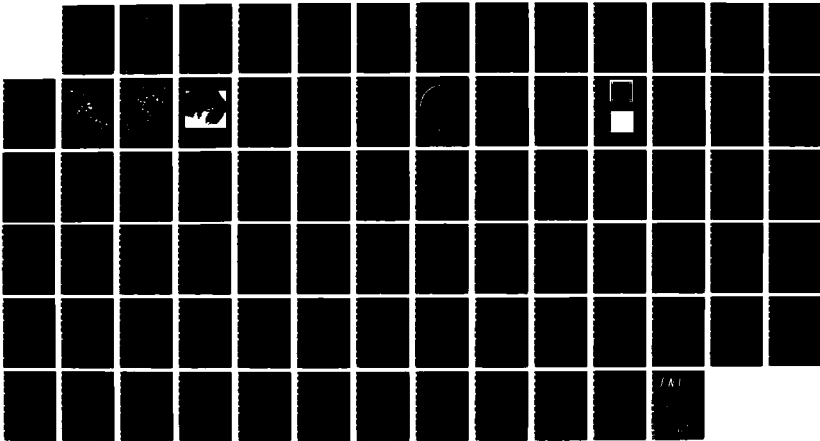
UNCLASSIFIED

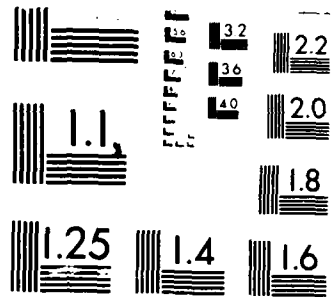
DEC 86 JPL-PUB-D-3041 DOT/FRA/CT-86/18

DTFA03-81-A-00765.

F/G 21/2

NL





MICROCOPY RESOLUTION TEST CHART
NATIONAL BUREAU OF STANDARDS

HART
A

2
②

DOT/FAA/CT-86/10

FAA TECHNICAL CENTER
Atlantic City Airport
N.J. 08405

AD-A178 255

Quantitative Determination of Engine Water Ingestion

P. Parikh
M. Hernan
V. Sarohia

Jet Propulsion Laboratory
California Institute of Technology
Pasadena, California 91109

December 1986

Final Report

This document is available to the U.S. public
through the National Technical Information
Service, Springfield, Virginia 22161.



US Department of Transportation
Federal Aviation Administration

OTC FILE COPY

87 3

NOTICE

This document is disseminated under the sponsorship of the Department of Transportation in the interest of information exchange. The United States Government assumes no liability for the contents or use thereof.

The United States Government does not endorse products or manufacturers. Trade or manufacturer's names appear herein solely because they are considered essential to the object of this report.

DISCLAIMER NOTICE

**THIS DOCUMENT IS BEST QUALITY
PRACTICABLE. THE COPY FURNISHED
TO DTIC CONTAINED A SIGNIFICANT
NUMBER OF PAGES WHICH DO NOT
REPRODUCE LEGIBLY.**

Technical Report Documentation Page

1. Report No. DOT/FAA/CT-86/10	2. Government Accession No.	3. Recipient's Catalog No.	
4. Title and Subtitle QUANTITATIVE DETERMINATION OF ENGINE WATER INGESTION		5. Report Date December 1986	
7. Author(s) P. Parikh, M. Hernan and V. Sarohia		6. Performing Organization Code	
9. Performing Organization Name and Address Jet Propulsion Laboratory California Institute of Technology 4800 Oak Grove Drive Pasadena, CA 91109		8. Performing Organization Report No. JPL Publication No. D-3041	
12. Sponsoring Agency Name and Address U.S. Department of Transportation Federal Aviation Administration Technical Center Atlantic City Airport, New Jersey 08405		10. Work Unit No. (TRAIS)	
		11. Contract or Grant No. DTFA03-81-A-00765	
		13. Type of Report and Period Covered Phase I May 84-Dec. 85	
15. Supplementary Notes Project Manager, Tom Rust, Engine/Fuel Safety Branch, Aircraft and Airport Safety Technology Division, FAA Technical Center			
16. Abstract This report describes a non-intrusive optical technique for determination of liquid mass flux in a droplet laden airstream. The technique was developed for quantitative determination of engine water ingestion resulting from heavy rain or wheel spray. Independent measurements of the liquid water content (LWC) of the droplet laden airstream and of the droplet velocities were made at the simulated nacelle inlet plane for the liquid mass flux determination. The liquid water content was measured by illuminating and photographing the droplets contained within a thin slice of the flow field by means of a sheet of light from a pulsed laser. A fluorescent dye introduced in the water enhanced the droplet image definition. The droplet velocities were determined from double exposed photographs of the moving droplet field. The technique was initially applied to a steady spray generated in a wind tunnel. It was found that although the spray was initially steady, the aerodynamic breakup process was inherently unsteady. This resulted in a wide variation of the instantaneous liquid water content of the droplet laden airstream. The standard deviation of ten separate LWC measurements was 31 percent of the average. However, the liquid mass flux calculated from the average LWC and droplet velocities came within 10 percent of the known water ingestion rate.			
17. Key Words ✓ Engine water, ingestion, wheel spray, Two-phase, flow measurement, aero- turbogas		18. Distribution Statement This document is available to U.S. Public through the National Technical Information Service, Springfield, Virginia 22161	
19. Security Classif. (of this report) Unclassified	20. Security Classif. (of this page) Unclassified	21. No. of Pages	22. Price

ACKNOWLEDGEMENTS

This work was sponsored at the Jet Propulsion Laboratory of California Institute of Technology by the U.S. Department of Transportation, Federal Aviation Administration Technical Center through NASA Contract NAS7-918, agreement No. DTFA03-81-A-00765. The authors extend their gratitude to Messrs. T. Rust, F. Howard, and W. T. Westfield of FAA Technical Center for their guidance and suggestions. The assistance of Messrs. W. Bixler and S. Kikkert in fabrication of the apparatus is gratefully acknowledged.



TABLE OF CONTENTS

	PAGE
EXECUTIVE SUMMARY	viii
INTRODUCTION	1
REVIEW OF APPLICABLE MEASUREMENT TECHNIQUES	1
PRESENT TECHNIQUE	2
WATER INGESTION SIMULATION FACILITY	8
IMAGE PROCESSING SYSTEM DESCRIPTION	10
RESULTS AND DISCUSSION	13
CONCLUDING REMARKS	17
REFERENCES	19
APPENDICES	
A. Image Analysis Program	A-1
B. Droplet Statistics Program	B-1
C. Droplet Data	C-1
D. Distribution List	D-1

LIST OF ILLUSTRATIONS

FIGURE		PAGE
1	Droplet Illumination and Photographic System	4
2	Droplet Photograph Without Fluorescent Dye in the Water	5
3	Droplet Photograph With Fluorescent Dye in the Water	6
4	Double Pulse Photograph of Droplets in a Moving Air Stream	7
5	Schematic Diagram of Engine Water Ingestion Simulation Facility	9
6	Typical Photograph of the Droplet Field at the Nacelle Inlet Plane	11
7	Image Processing System Architecture	12
8	Digital Subimage Representing One Grid Square	14
9	Enhanced Version of Digital Subimage Shown in Figure 9	14
10	Droplet Size Distribution at the Nacelle Inlet Plane	18

NOMENCLATURE

A_f Frontal area of nacelle. (m^2)
D Droplet Diameter (mm)
LWC Liquid Water Content (gm/m^3)
 m_w Mass flow rate of water (gm/sec)
n Number of drops counted
q_w Total liquid volume in the measurement volume (cm^3)
Q_w Volumetric water ingestion rate (cm^3/sec)
V_a Airspeed (m/sec)
V_w Water jet speed at the spray nozzle (m/sec)
V_d Average water drop speed (m/sec)
x distance downstream from the spray nozzle (m)

Greek Letters

ρ_w Water density (gm/cm^3); 1.0 gm/cm^3
 δ Thickness of the Light Sheet (mm)

Subscripts

a Average spray property
i Identify ith drop, where i = 1 to n

EXECUTIVE SUMMARY

Water droplet ingestion into turbine engines resulting from heavy rain and wheel spray generated on a wet runway is of importance. Adverse effects of large quantities of water ingestion can include the compressor stall and combustor flame-out. Engine certification requirements as set forth in FAA regulations call for continued engine operation at takeoff and flight idle conditions while ingesting water at 4 percent by weight of airflow, generated by a spray to simulate rain. There is also a certification requirement on the entire aircraft system which dictates that the system must be designed to prevent hazardous quantities of water from being ingested into the engine during takeoff, landing and taxiing operations on wet runways. The present work was undertaken to develop measurement techniques of two-phase droplet laden airstreams during engine water ingestion. The ultimate objective is to correlate the non-intrusive measurements of the water ingestion rate and droplet size and spatial distribution at the engine inlet with engine performance parameters. Such techniques and data will assist the FAA in evaluating current water ingestion certification tests.

A non-intrusive optical technique was developed for the determination of liquid mass flux in a droplet laden airstream. The technique is also capable of providing information on the droplet size and spatial distribution at the nacelle inlet plane.

Independent measurements of the liquid water content (LWC) of the droplet laden airstream and of the droplet velocities were made at the inlet plane of a simulated nacelle in a wind tunnel for the liquid mass flux determination. The liquid water content was determined by illuminating and photographing the droplets contained within a thin slice of the flow-field by means of a sheet of light from a pulsed laser. Fluorescent dye introduced in the water enhanced the droplet image definition. The droplet velocities were determined from double exposed photographs of the moving droplet field. The technique was initially applied to a steady spray generated in a wind tunnel. It was found that although the spray was initially steady, the aerodynamic breakup process was inherently unsteady. This resulted in a wide variation of the instantaneous liquid water content of the droplet laden airstream. The standard deviation of ten separate LWC measurements was 31 percent of the average. However, the liquid mass flux calculated from the average LWC and droplet velocities came within 10 percent of the known water ingestion rate.

INTRODUCTION

The effects of water droplet ingestion into turbine engines resulting from heavy rain and wheel spray generated on a wet runway is of importance. The effects of water ingestion on engine performance have recently been investigated (reference 1) and a probe for stagnation pressure measurement in a droplet laden airflow was developed (reference 2). The adverse effects of large quantities of water ingestion can include the compressor stall and combustor flame-out (reference 1). Engine certification requirement as set forth in FAA regulations (reference 3) call for continued engine operation at takeoff and flight idle conditions while ingesting water at 4 percent by weight of airflow, generated by a spray to simulate rain. There is also a certification requirement on the entire aircraft system which dictates that the system must be designed to prevent hazardous quantities of water from being ingested into the engine during takeoff, landing, and taxiing operations, (reference 4).

The criteria for both water ingestion certification tests are somewhat arbitrary. The 4 percent by weight water ingestion test for engine certification does not address such issues as droplet size and their spatial distribution over the frontal area of the nacelle. For performance on a wet runway, the criterion is even more arbitrary in that it does not specify what constitutes a hazardous quantity of water ingestion.

The present work was undertaken to develop measurement techniques in two-phase droplet laden airstreams to better quantify the engine water ingestion. The ultimate objective is to correlate non-intrusive measurements of the water ingestion rate and droplet size and spatial distribution at the engine inlet with engine performance parameters. Such techniques and data will assist the FAA in evaluating current water ingestion certification tests.

REVIEW OF APPLICABLE MEASUREMENT TECHNIQUES

A review of available measurement techniques for sprays was undertaken to determine the applicability of the existing techniques to quantitative determination of water ingestion into an engine. The quantities that need to be determined are:

- a) Drop size distribution together with spatial distribution of drops at the nacelle inlet.
- b) The mass flow rate of water crossing the nacelle inlet plane at any instant.

Extensive work on measurements of wheel sprays generated by aircraft under-carriages was carried out by Barrett (reference 5). A spray intensity probe was developed to measure mean local dynamic pressure generated by moving droplets. However, all of Barrett's measurements were in the near field of the wheel generating the spray and the technique used only provided time averaged local measurements in the spray.

Several mechanical, electrical, and optical methods are available for droplet size determination in fuel sprays as surveyed in review articles by Jones

(reference 6) and, McCreathe and Beer (reference 7). None of the techniques surveyed would be capable, in their existing form, of satisfying the second requirement above. It was considered possible that the requirement could be met by some modification of the existing techniques.

The first trial approach was an extension of the charged wire probe technique described by Gardiner (reference 8) for drop size determination in water sprays. In that technique, the electrical pulse generated in a circuit containing a charged electrode when a drop impacts the electrode is measured by a pulse height analyzer. The probe is initially calibrated using known size drops impacting the electrode. A relationship is established between the pulse height and the drop size. In practice, the drop size characteristics are derived from the pulse height statistics stored in a pulse height analyzer. The technique as described by Gardiner (reference 8) thus provides the local drop size distribution in a spray. In the present work, a modification of the technique was considered. Instead of a single electrode probe, a charged grid was considered. A copper wire mesh with wire spacing of approximately 1 mm was charged to 2000 volts by a high voltage DC power supply. The idea was to install the screen at the nacelle inlet plane so that all drops larger than the mesh size would be intercepted by the screen. The charge transfer between the screen and the impacting drops would set up a current in the circuit supplying the grid. The current would be proportional to the total surface area of the drops impacting per unit time. Then if the size distribution were to be determined by an independent optical technique, the volume flow rate of water would be proportional to the product of the Sauter Mean Diameter (SMD) of the spray and the current supplied to the grid.

In practice, however, several difficulties were encountered with this technique.

- 1) The charge distribution on the screen was non-uniform, resulting in different pulse characteristics for different impact locations on the screen for the same size drop.
- 2) Wetting of the screen altered the initial charge distribution.
- 3) Water film on the support set up a conduction path from the screen to the ground, causing a leakage current.

Because of these difficulties and the fact that an optical technique was still needed in conjunction with the charged screen for water flow determination, this approach was abandoned in favor of a purely optical non-intrusive technique.

PRESENT TECHNIQUE

A non-intrusive optical technique was developed for the determination of drop sizes, spatial distribution of drops at the nacelle inlet plane and instantaneous mass flow rate of liquid water entering the nacelle. The liquid water mass flow rate is determined by independent measurements of the liquid water content of the droplet laden airstream and the droplet velocity at the nacelle inlet plane.

For liquid water content (LWC) determination, a thin cross-section of the flow close to the nacelle inlet plane is illuminated by a pulsed laser light sheet. The drops contained within this light sheet are photographed by a camera placed with its axis nearly normal to the plane of the light sheet (figure 1). The duration of illumination of drops by the laser pulse is extremely short, about 10 nano second. Therefore, the motion of the drops is frozen in the photographs. The thickness of the laser sheet is controlled by a beam expander and a slit. The slit was of 9 mm width while the initial beam width was 14 mm. The slit thus allowed only the intense central portion of the expanded beam to pass through, cutting off the less intense outer portions.

The depth of field of the camera is set to be larger than the light sheet thickness by proper selection of aperture and magnification. This assures that all illuminated drops (contained within the light sheet) appear in the photographs with a sharp edge definition. The measurement volume is defined by the product of the projected frontal area of the nacelle and the light sheet thickness. Information on drop sizes and spatial distribution is also obtained from this photograph.

When drops are photographed using the optical set up as shown in figure 1, with proper focusing and depth of field selection, the droplet edge definitions in the resulting photographic images are still far from ideal as shown in figure 2. This is caused by two effects:

- 1) The illumination of individual drops is not uniform, resulting in poor image definition of larger drops.
- 2) Scattering and diffraction around smaller drops causes a "halo" effect around the drop boundary, causing the image to appear much larger than the actual size.

An improved version of this technique utilizes laser induced fluorescence of a small quantity (less than 10 ppm) of dye (Rhodamine 6G or Fluorescene) introduced in the water. The fluorescence spectrum of the dye lies in a wavelength range longer than that of the incident light, therefore, the incident light scattered from the drops can be filtered out and only the fluoresced light is photographed. Shott colored glass filters are ideally suited for this purpose. This technique results in much better edge definition of droplets in the photographic images and a nearly uniform illumination of droplet interior (see figure 3).

An automated digital image processing system was developed to analyze the photographic images. The image processing algorithm detected drop edges, defined droplet boundaries, calculated the area of the drop images and an equivalent drop diameter based on this area. Droplet size distributions were constructed once statistics on a sufficient number of drops were available. The liquid water content was determined from the total volume of drops contained within the projected area of the nacelle, together with the knowledge of the incident light sheet thickness. A description of the image processing system is presented later in this report.

For the determination of instantaneous mass flow rate of airborne liquid water, a measurement of drop velocities is needed in addition to the LWC measurement. This may be accomplished non-intrusively by laser double pulse photography of the moving droplet field. Two images of each drop appear in the photograph (see figure 4) and the drop velocity may be determined by the measurement of

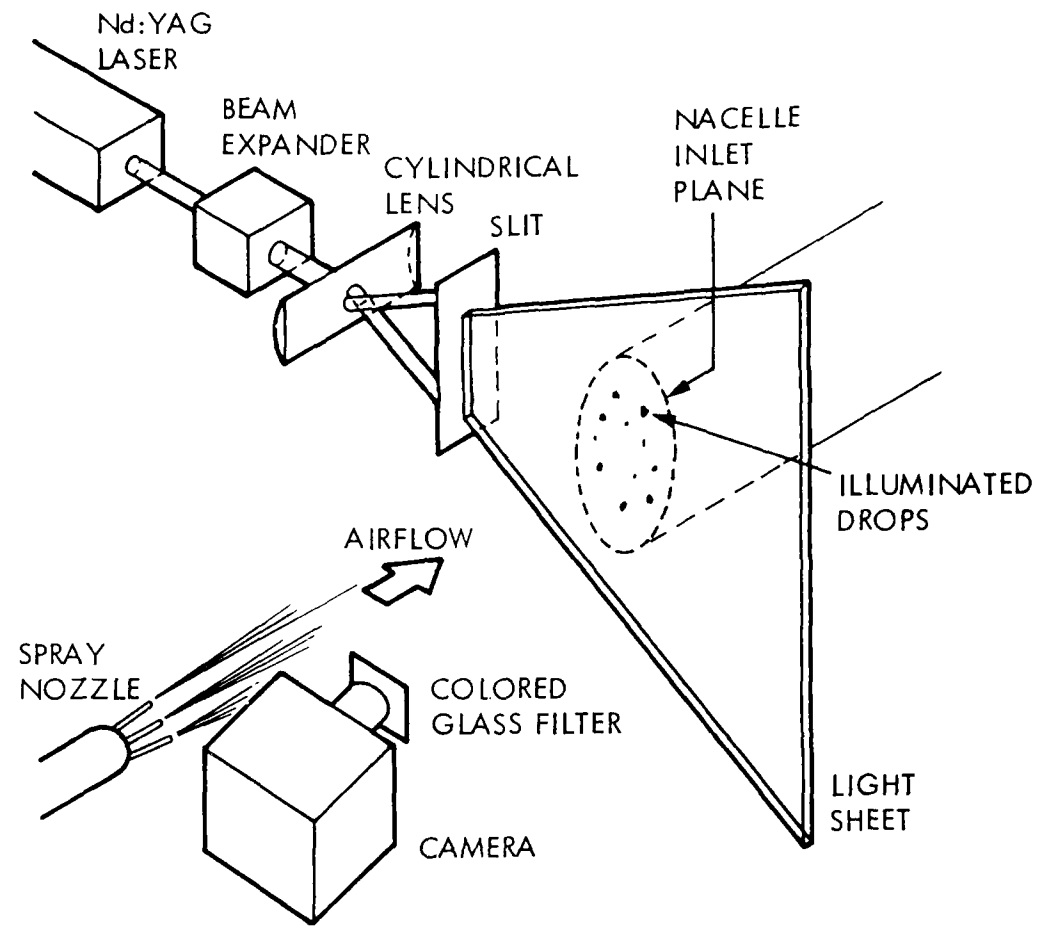


Figure 1. Droplet Illumination and Photographic System



Figure 2. Droplet Photograph Without Fluorescent Dye in the Water

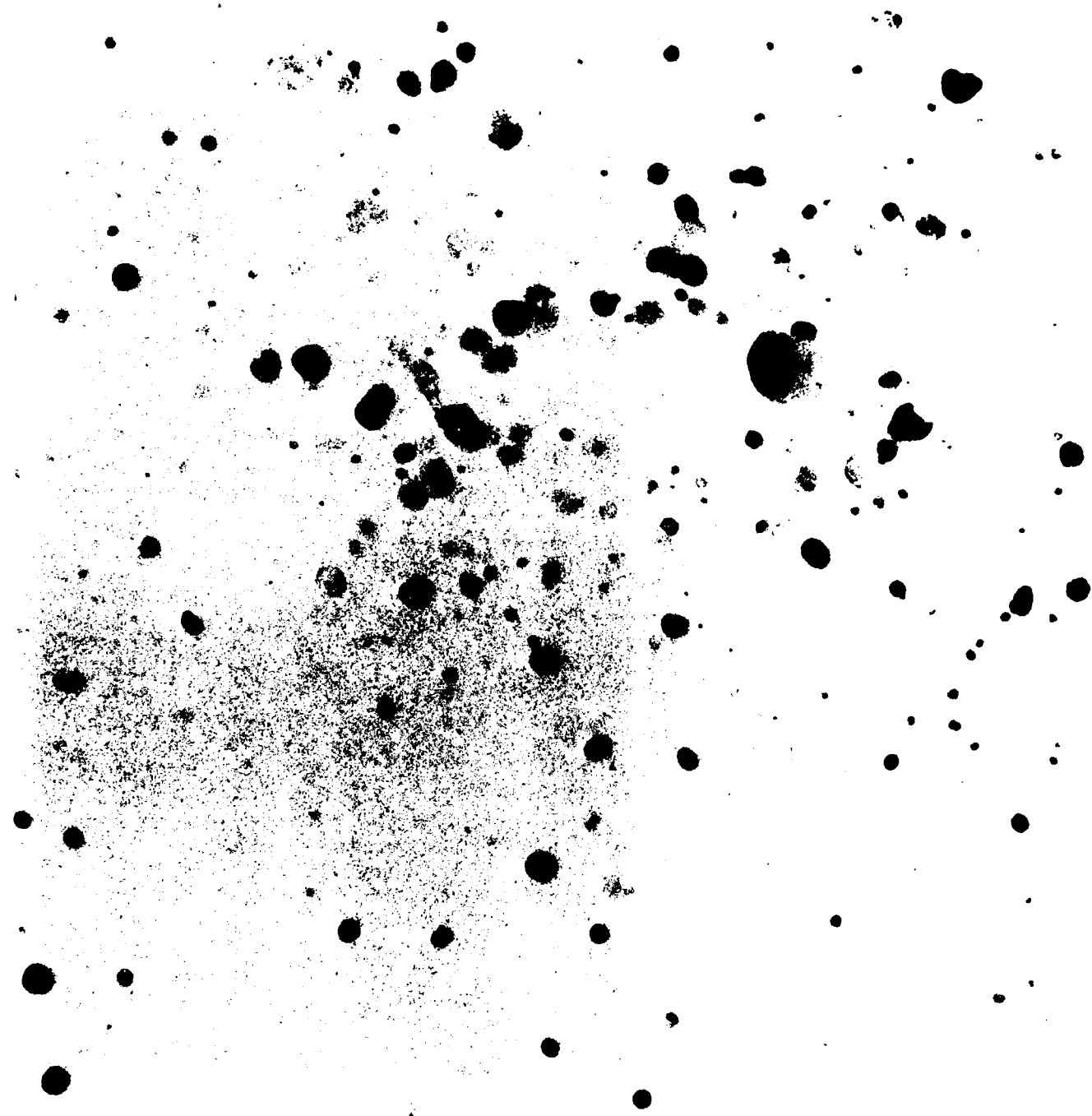


Figure 3. Droplet Photograph With Fluorescent Dye in the Water



Figure 4. Double Pulse Photograph of Droplets in a Moving Air Stream

the distance translated in a known time interval. Solid-state lasers such as Ruby or Neodymium: yttrium aluminum garnet (Nd:YAG) lasers may be operated in the double pulse mode, wherein the Q-switch is opened twice in rapid succession to split the energy of the flash tube between two intense pulses. The time interval between the two pulses may be adjusted in the range of 50 to 200 μ s.

The product of the LWC evaluated over the nacelle frontal area, the drop velocity and the nacelle frontal area is the instantaneous mass flow rate of airborne liquid water into the nacelle.

WATER INGESTION SIMULATION FACILITY

In the first phase of the program, an experimental facility was developed to simulate engine water ingestion and to calibrate the non-intrusive optical technique for the quantitative measurements of engine water ingestion. A description of the facility follows.

The engine water ingestion simulation was set up in an open circuit wind tunnel of 18-inch x 18-inch test section. A schematic diagram of this facility is shown in figure 5. Air was supplied to the test section by a high capacity blower via a settling chamber, screens and a nozzle contraction. The blower output was adjusted by a damper vane ring at the inlet. A water spray nozzle was mounted on a streamlined sting support at the entrance to the test section. The nozzle consisted of seven 2 cm long tubes of 1.6 mm inside diameter. The water was supplied to the nozzle from a pressurized tank via a flowmeter and a ball valve. The individual tubes of the spray nozzle were adjusted such that most of the spray water entered the simulated nacelle with the tunnel running. The droplet-air mixture entering the simulated nacelle passed through a separator box which contained a series of baffle plates. The baffle plates subjected the flow to a series of sharp turns, thereby separating the droplets from the airstream and collecting them in a water film on the plate surfaces. Most of the water entering the nacelle in the form of droplets was collected at the bottom of the separator box. The air was evacuated from the separator box by means of the suction provided by the inlet of a secondary blower. The air from the exit side of the secondary blower was dumped back into the tunnel, downstream of the nacelle location. Calibration checks were made to determine the carry over loss of water in the form of fine drops. For the spray flow rate employed (300 cc/sec), the carry over loss was about 5 percent, with 95 percent of the water sprayed into the nacelle being collected at the bottom of the separator. With a steady spray, the total mass of water collected, divided by the time of collection was close to the time averaged mass flow rate of water entering the nacelle in the droplet-air mixture.

The optical set up is shown in figure 1. The laser sheet of 9 mm thickness was produced in front of the nacelle inlet plane approximately 2 mm from the inlet plane to avoid illuminating the water film on the rounded nacelle entrance. The illuminated droplet field was viewed through the side of the tunnel. The camera axis formed an angle of approximately 20 degrees with the nacelle axis. In viewing the droplet field through the plexiglas wall of the tunnel at such a shallow angle, multiple reflections of illuminated drops were encountered within the plexiglas wall. To alleviate this problem, a window extension was mounted on the tunnel side wall at a 20 degree angle, such that the camera line of sight was normal to the window at the end of the extension.

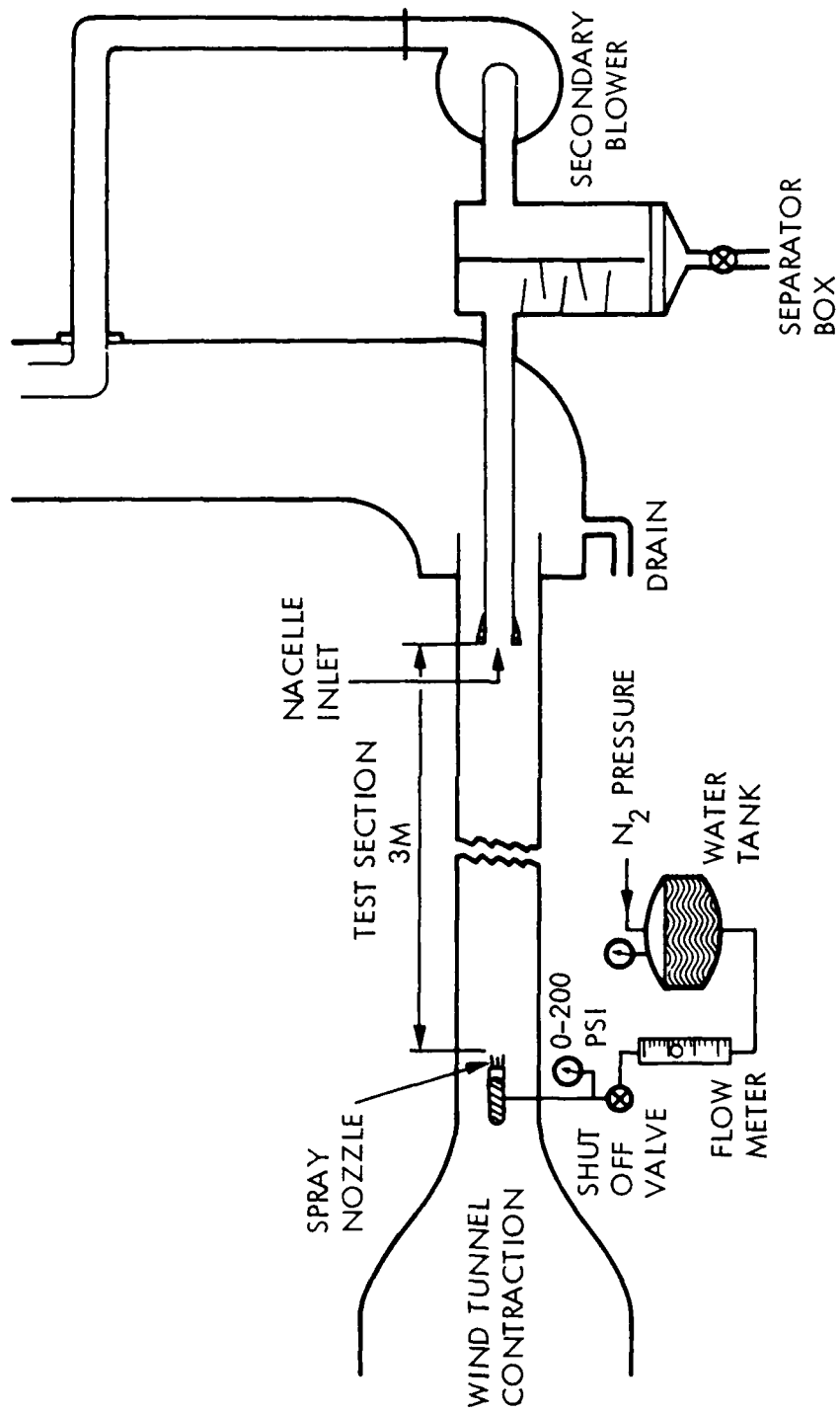


Figure 5. Schematic Diagram of Engine Water Ingestion Simulation Facility

The objective of the experiments was to compare the instantaneous water flow rate into the nacelle as determined by the present non-intrusive optical technique with the known time averaged water flow rate. Ten photographs were taken for a fixed spray rate and airspeed to yield a set of ten successive LWC measurements in a steady spray. The variation in the drop velocities within a given double exposed photograph or between two photographs at fixed tunnel speed and water injection pressure was found to be less than 5 percent. Therefore, a single drop velocity was used for water mass flow rate determination. A sample photograph of droplet field is shown in figure 6. The nacelle boundary was photographed separately and superimposed onto the droplet photograph in figure 6. Notice that the drops within the light sheet are uniformly illuminated and appear with sharp boundaries. Unfortunately, due to light scattered from drops contained in the light sheet and that from the beam dump and the transmitting side plexiglas window, some of the drops outside the laser sheet appear with faint images. During image processing of the photographic negatives, these faint drops, which are present outside the light sheet may easily be eliminated by setting proper threshold criteria.

IMAGE PROCESSING SYSTEM DESCRIPTION

Processing system architecture is depicted in figure 7. Image acquisition, display and processing was accomplished using a De-Anza ID-5400 image processing system. The hardware package incorporates a vidicon and power supply for analog image formation, three image refresh random access memory channels, RAM, digital video array processor, and color video display. The analogue signal from the video camera can be digitized by an A/D converter and fed directly to the array processor which in turn controls the data flow and writes the data into one of the memory planes at a rate of 30 frames/sec. The digitization process converts each picture into 512*512 matrix element (pixels). Each pixel is one byte number (256 resolution level) representing the average optical density in an elementary cell, the size of which dictates the spatial resolution of the system. While digitization can proceed at video rates of 30 frames per second, a program is used which creates one digital frame from the average of 64 consecutive digitized frames. Thus, the image formed has a low level of random noise caused by the vidicon and the digitizer electronics. The digitized image information is then stored on a mass-storage device for further off-line processing.

Software residing in the host computer (PDP 11/34) operates through a direct memory access (DMA), interface through which the PDP-11 sends and receives information from the video processor registers or from the RAM channels via a driver program. The vidicon image digitization, averaging and storage capability is part of this (DMA) interface software.

To study a droplet picture, the negative is taped on to a transparency containing a 1 cm x 1 cm grid formed by fine lines. The grid lines are carefully oriented with respect to the droplet images on the negative such that none of the drop images is intersected by the grid lines. The negative, together with the grid lines, is then mounted on a flat light-table. The vidicon is focused on the plane of the background illuminated negative by means of a macro lens. The magnification on to the vidicon is adjusted such that a 1 cm^2 area of the negative enclosed by the superposed grid lines nearly fills a video frame containing the 512 x 512 pixel array. After accounting for the photographic magnification of the image on the negative and a specification of

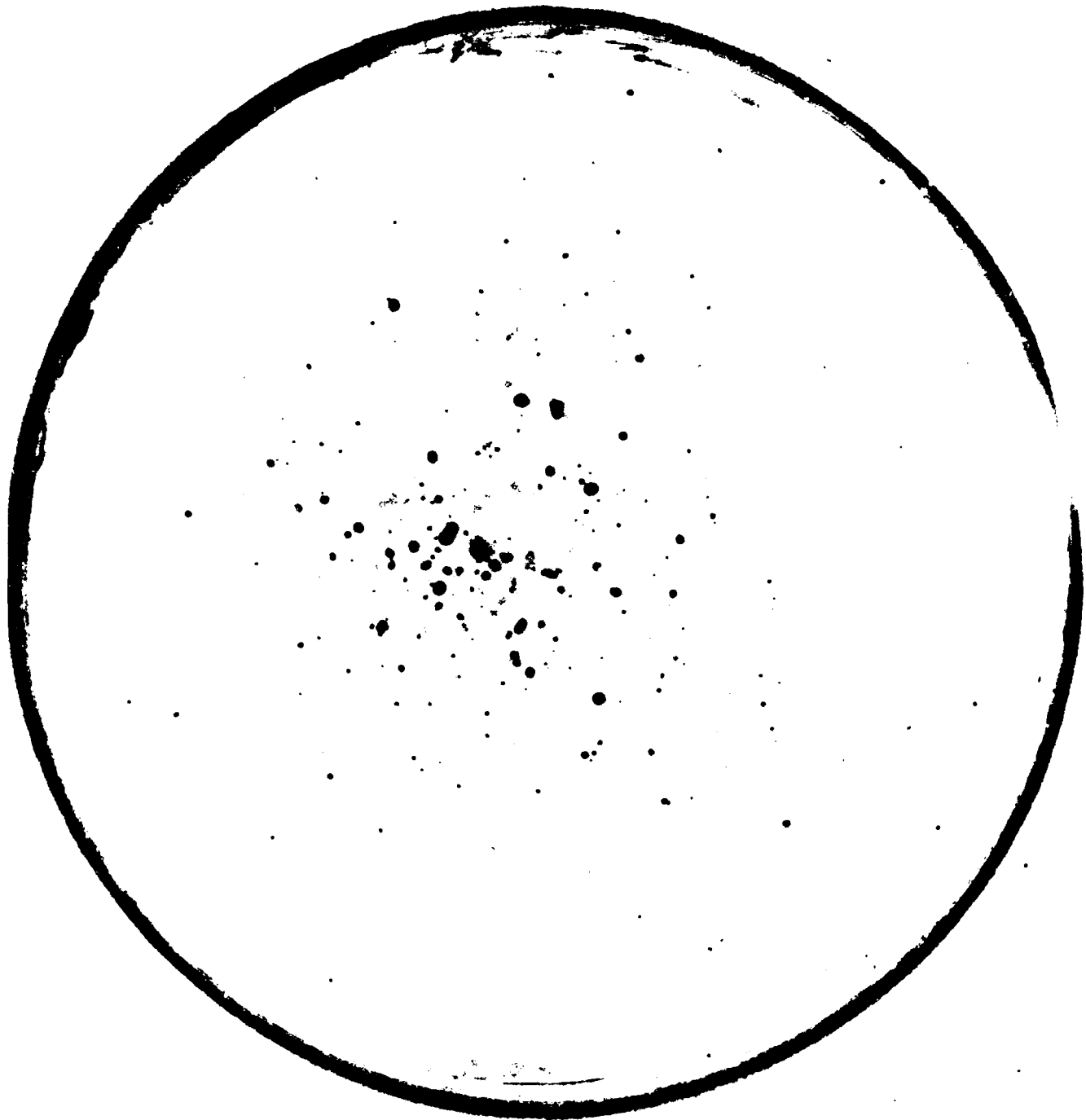


Figure 6. Typical Photograph of the Droplet Field at the Nacelle inlet plane

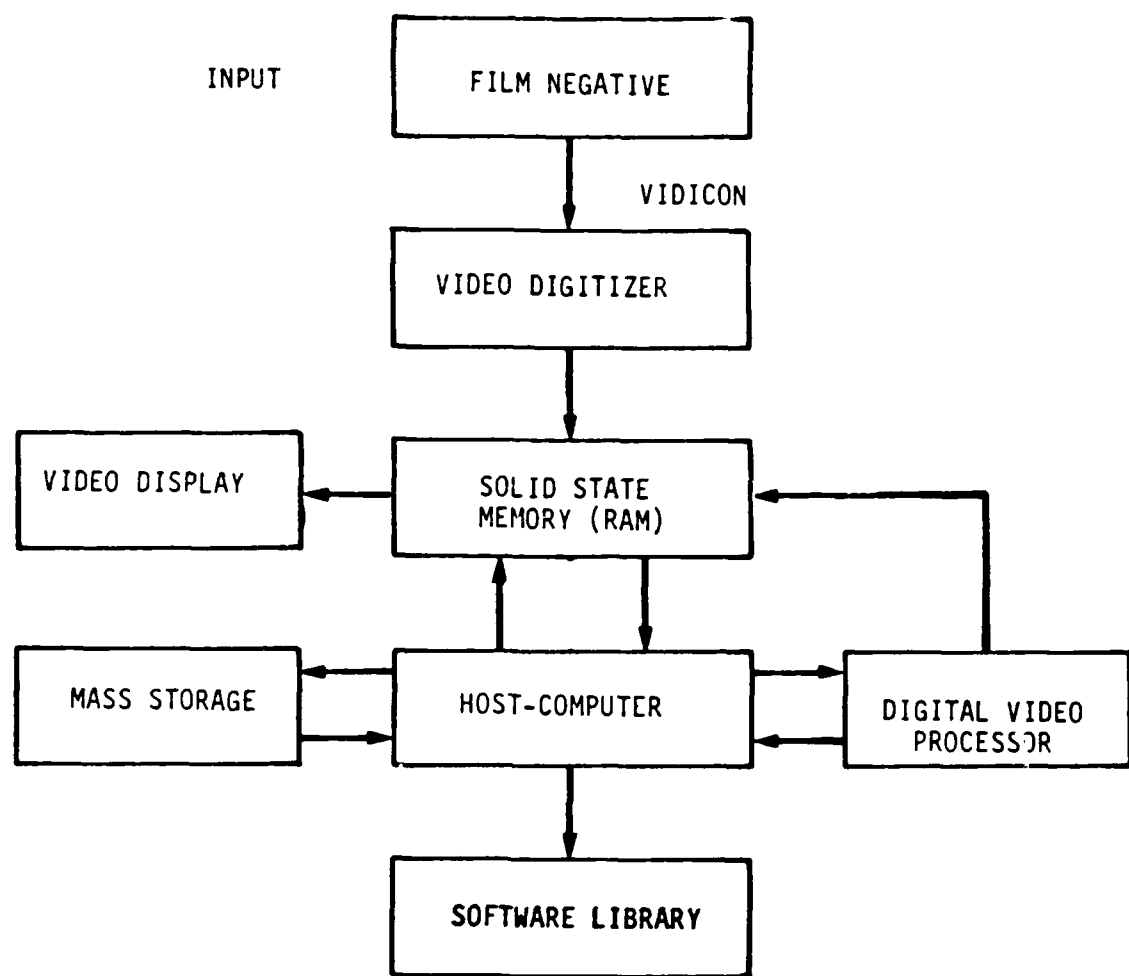


Figure 7. Image Processing System Architecture

4 pixels for the minimum size drop accepted, an overall resolution of 0.1 mm was estimated for the diameter of the smallest drop measured.

The negative was scanned, one grid square at a time over the projected frontal area of the nacelle. The calculated drop volumes were then added up for all the squares to evaluate the liquid water content over the projected frontal area of the nacelle. This procedure ensured that every drop is accounted for and is counted only once. An example of a digital subimage representing one grid square is shown in figure 8. An enhanced image with defined droplet boundaries is shown in figure 9.

Image processing software was developed to detect drop edges, define droplet boundaries, and calculate the area of drop images. The excellent contrast between the images of drops within the light sheet and the background allowed a simple thresholding criterion to define regions containing drop images.

The various image processing programs along with computer program needed for droplet statistics determination are attached under Appendices A and B, respectively.

RESULTS AND DISCUSSION

Results are presented here for fixed values of spray flow rate and airspeed in the wheel spray simulation tunnel. The flow rate through the spray nozzle was maintained constant at 0.3 liters/sec, which resulted in a water jet velocity of 22 m/s based on the total flow area of the seven tubes in the spray nozzle. As discussed later, this flow rate was chosen to simulate extreme cases of engine water ingestion resulting from wheel spray. The airspeed was maintained at 61 m/s. The large difference between the speeds of the air and the water jets caused an aerodynamic breakup of the water jets into small drops, which accelerated along the flow direction to approach the airspeed. The measurement station was located 3 m downstream of the spray nozzle and immediately upstream of the simulated nacelle inlet.

The droplet velocities were determined from a double exposed photograph of the moving droplet field as shown in figure 4. A 100 μ s time interval between the two pulses was employed. The droplet velocities were found to be within 5 percent for a large number of droplet pairs. Furthermore, within this small variation of droplet velocities, no correlation was found between the drop velocity and size. A single average value of velocity was assigned to all droplets. This average value was found to be only 41 m/s, i.e., 67 percent of the airspeed. Thus, the 3 m distance between the spray nozzle and the measurement station was insufficient to accelerate the drops to the tunnel airspeed.

A series of ten photographs was taken during the period January-February 1986 for the liquid water content determination. The width of the light sheet was maintained at 9 mm. The photographic negatives were analyzed by the image processing technique discussed in this report. The volume of a drop was calculated as the volume of a spherical drop having the same equivalent diameter. The equivalent diameter was calculated from the image area of each drop. For a non-spherical drop this procedure leads to a higher value of the calculated drop volume. The percentage error introduced therefore depends upon the how different the drop is as compared to the spherical shape.

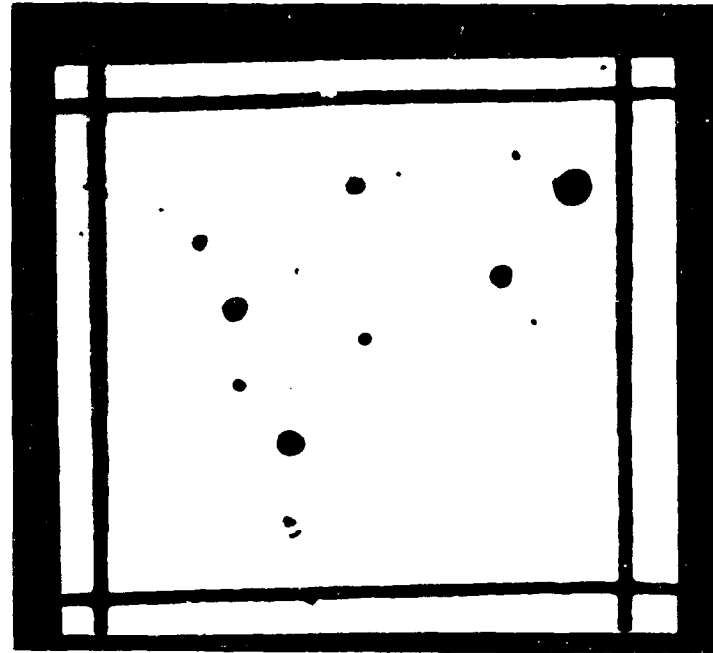


Figure 8. Digital Subimage Representing One Grid Square

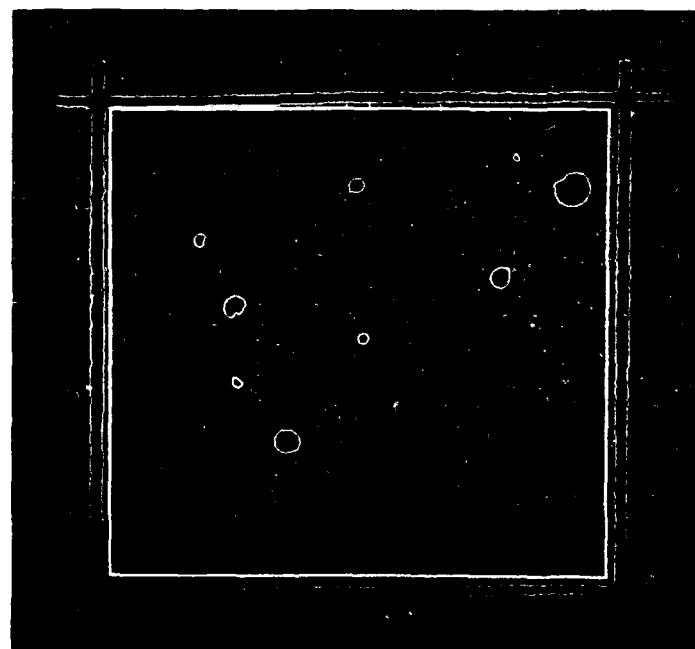


Figure 9. Enhanced Version of Digital Subimage Shown in Figure 8

The results of the image processing analysis are shown in table I. The raw droplet data has been shown under Appendix C. For each of the ten droplet pictures analyzed, the total number of drops counted over the nacelle frontal area, the mean droplet diameter, the volume weighted mean diameter and the total liquid volume are presented. The standard deviation of the mean and volume weighted mean droplet diameters as calculated from the ten pictures was in the range of 7 to 8 percent of the average. This indicated that the picture-to-picture variation of the calculated mean diameter was relatively small. The picture-to-picture variation of the total liquid volume was larger: the standard deviation of the ten measurements was 31 percent of the average. The average value of the total liquid volume from the ten pictures was used to calculate the average liquid water content, i.e.,

$$(LWC)_a = \frac{\rho_w q_w}{A_f \cdot \delta} = 450 \text{ gm/m}^3; \text{ where } \rho_w = 1.0 \text{ gm/cm}^3$$

The average mass flow rate of water was then calculated as

$$\dot{m}_w = (LWC)_a \cdot A_f \cdot V_d$$

$$= 332.5 \text{ gm/sec}$$

The average mass flow rate of water in the moving droplet-air mixture as measured by the present non-intrusive optical technique thus indicates a flow rate approximately 10 percent higher than the actual value of 0.3 l/s. Reasons for this discrepancy between the measured and the actual mass flow rates are discussed below. It should be noted however, that there is a significant picture-to-picture variation in the instantaneous water mass flow rate determinations caused by measured variations in the instantaneous LWC values. The test droplet spray was quite dense in comparison with the certification requirement of 4 percent by weight of liquid water in the airstream. The present 0.3 l/s water ingestion rate in a 61 m/s airstream over the frontal area of the 15.24 cm diameter nacelle translates to a water flow rate/airflow rate ratio of 22.5 percent. Such a high water spray rate was used to simulate extreme cases of engine water ingestion resulting from wheel spray.

There are three factors that affect the accuracy of LWC measurement by the present technique:

- 1) Droplets largely outside the light sheet but at the boundary are partially grazed by the light sheet and show up on photographs, thus increasing the LWC measured.
- 2) The procedure for calculation of drop volume from its non-spherical images on the photograph relies on an equivalent diameter which is calculated from the enclosed area of the image. This procedure tends to over-predict the volume of the non-spherical drop and hence leads to a higher value of measured LWC.
- 3) The illuminated drops contained in the light sheet are viewed by the camera through a dense spray. Therefore, there is a possibility of some illuminated drops being masked by droplets present in the view path of the camera. This masking will result in a lower value of the measured LWC.

TABLE I
Summary of Data Photographs

$V_a = 61 \text{ m/s}$; $V_w = 21.7 \text{ m/s}$; $Q_w = 300 \text{ cm}^3/\text{sec}$; $x = 3 \text{ m}$; $A_f = 182.4 \text{ cm}^2$;
 $\delta = 9 \text{ mm}$

Negative No.	No. of Drops	Mean Dia. mm	Vol. Mean Dia. mm	Total Liquid Vol. mm ³
1	267	0.55	0.89	97.4
2	207	0.58	0.86	68.2
3	256	0.51	0.87	89.0
4	155	0.58	0.86	52.3
5	179	0.63	0.92	88.0
6	212	0.56	0.88	75.0
7	243	0.59	0.91	95.7
8	128	0.50	0.68	21.5
9	337	0.53	0.80	91.8
10	169	0.60	0.87	57.8
Average:		0.56	0.85	73.7
Standard Deviation:		0.04	0.066	23.0
Std Dev. percent of Mean:		7.0	7.8	31.0

NOTE: Mean Dia. = $\frac{\sum n_i D_i}{\sum n_i}$; Vol. Mean Dia. = $\frac{\sum n_i D_i^4}{\sum n_i D_i^3}$

$$\text{Total Liquid Vol.} = \sum n_i \frac{\pi}{6} D_i^3$$

Despite these three sources of errors, the present non-intrusive technique is still considered a good method for measurement of the liquid water flow rate in a moving droplet-laden airstream.

The droplet size distribution determined from the more than 2000 drops counted in the ten pictures is shown in figure 10.

CONCLUDING REMARKS

- 1) A non-intrusive optical technique has been developed for quantitative determination of instantaneous liquid water mass flow rate in a droplet laden airstream. The technique is generally applicable to the problem of water ingestion into an engine resulting in up to 22% water by weight (rain or wheel spray).
- 2) The technique yields instantaneous spatial distribution of droplets at the nacelle inlet plane as well as the droplet size distribution.
- 3) Significant variation in the instantaneous values of the liquid water content was encountered in a droplet laden airstream produced by injection of a steady water spray in a steady airstream. The standard deviation among ten separate instantaneous determinations of the LWC was 31 percent of the average LWC.
- 4) The average liquid water flow rate as determined from the average LWC and drop velocity measurements was approximately 10 percent higher than the actual spray flow rate.

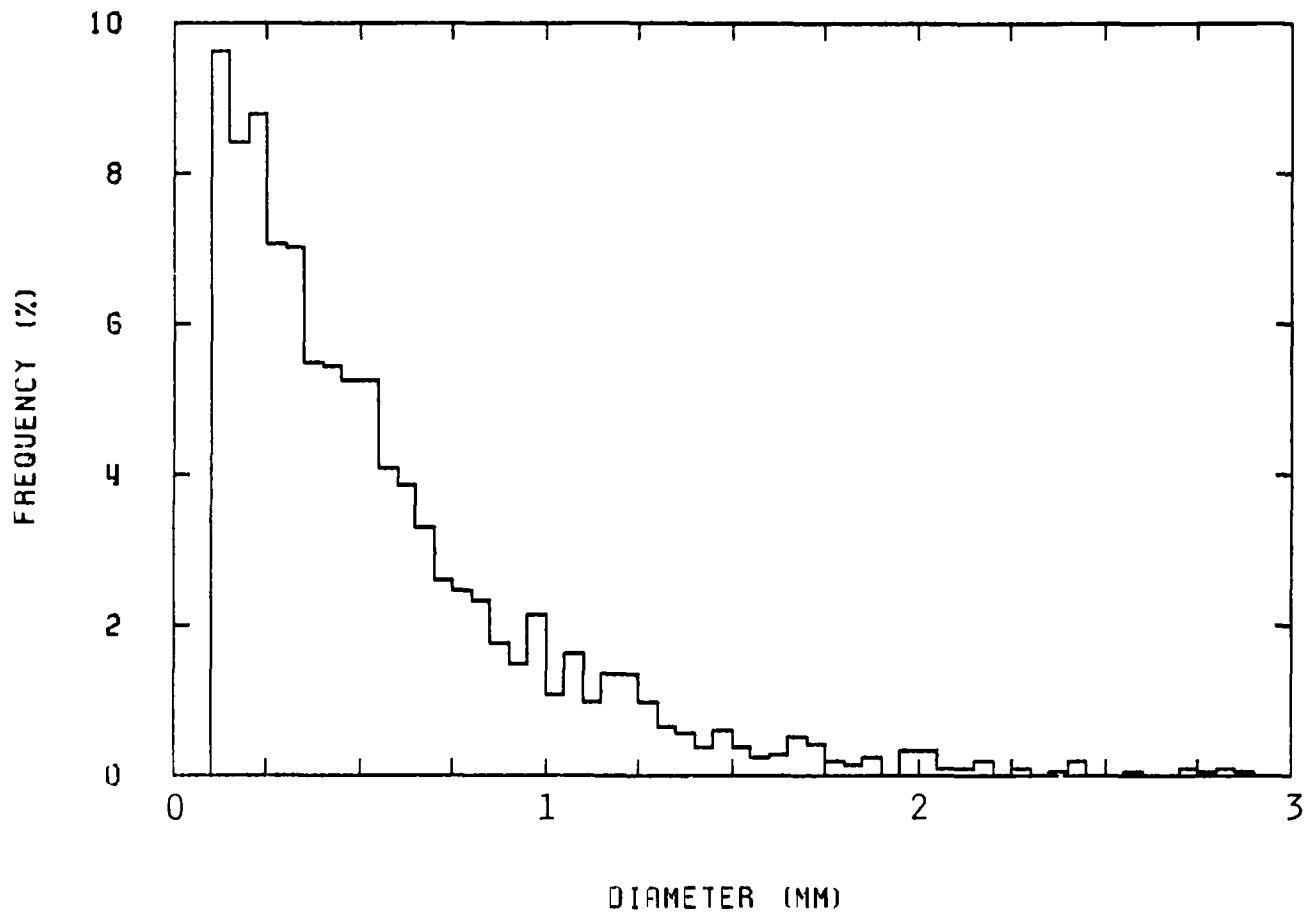


Figure 10. Droplet Size Distribution at the Nacelle Inlet Plane

REFERENCES

1. Murthy, S.N.B. and C.M. Ehresman: Effects of Water Ingestion into Jet Engine. AIAA paper No. 84-0542 presented at the Airbreathing Propulsion Session of the 22nd Aerospace Sciences Meeting, January 1984.
2. Murthy, S.N.B. et.al.: A Stagnation Pressure Probe for Droplet-laden Air Flow. AIAA paper No. 85-0330 presented at the Airbreathing Propulsion Session of the 23rd Aerospace Sciences Meeting, January 1985.
3. Code of Federal Regulations, Title 14-Aeronautics and Space, Chapter 1-Federal Aviation Administration, Article 33.77, paragraphs (c) and (f). January 1980.
4. Code of Federal Regulations, Title 14-Aeronautics and Space, Chapter 1-Federal Aviation Administration, Article 25.1091, paragraph (d)(2). January 1980.
5. Barrett, R.V.: Spray From Aircraft Undercarriages at High Speed - a Model Investigation. The Aeronautical Journal, Royal Aeronautical Society, May 1977.
6. Jones, A.R.: A Review of Drop Size Measurement - The Application of Techniques to Dense Fuel Sprays. Progress in Energy and Combustion Science. Vol. 3. 1977.
7. McCreath, C.G. and J.M. Beer: A Review of Drop Size Measurement in Fuel Sprays. Applied Energy, Vol. 2. 1976.
8. Gardiner, J.A.: Measurement of the Drop Size Distribution in Water Sprays by an Electrical Method. Instrument Practice. April 1964.

APPENDIX A

IMAGE ANALYSIS PROGRAMS

FORTRAN IV-P V82-51 10:58:17 26-APR-85 P 1
DROPS.FTN /TR:BLOCKS/WR

0001 PROGRAM DROPS
C
C Drops analysis based on averaged maximum gradient
C
0002 LOGICAL*1 ANSA,ANS0
0003 BYTE ZERO
0004 REAL*8 HIST(0:256),DMAXQ
0005 BYTE BUPIC(512),BUGRA(512)
0006 BYTE PIXEL(512,16)
0007 COMMON/PINTA/PIXEL
0008 INTEGER*2 IVLT(256)
0009 INTEGER*2 ARMIN
0010 INTEGER*2 IBUFO(8) ! Basic data processing parameters
0011 EQUIVALENCE (IBUFO(1),KREDC)
0012 EQUIVALENCE (IBUFO(2),SCALE)
0013 EQUIVALENCE (IBUFO(4),ARMIN)
0014 EQUIVALENCE (IBUFO(5),ICORTA)
0015 INTEGER*2 SL,SS,NL,NS
0016 REAL*4 ABUF(200),PBUF(200)
0017 INTEGER*2 LINIT(4,200)
0018 COMMON/MINARE/AMINAR
0019 INTEGER*2 IBUFE(3),PL,PC,CL,CC
0020 REAL*4 AREA,PERIM
0021 EQUIVALENCE (IBUFE(1),PL)
0022 EQUIVALENCE (IBUFE(2),PC)
0023 EQUIVALENCE (IBUFE(3),CL)
0024 EQUIVALENCE (IBUFE(4),CC)
0025 EQUIVALENCE (IBUFE(5),AREA)
0026 EQUIVALENCE (IBUFE(7),PERIM)
C
C
C Open data file
C
0027 OPEN (UNIT=3,NAME='SY:[300,300]RAIN.DAT',TYPE='OLD',
1 DISP='KEEP',ACCESS='DIRECT',RECORDSIZE=4,FORM='UNFORMATTED')
0028 READ(3,11) IBUFO
0029 IF (KREDC.NE.0) GO TO 900
0030 KREDC=11 Initial record for parameters storage,no data
0031 ARMIN=51 Default min area
0032 ICORTA=5
0033 SCALE=1
0034 TYPE *, ' Processing parameters initialization, defaults are:'
0035 TYPE *, ' Min area 5 Sq. pixels, Scale 1 mm/pixel; Change (Y/N)?'
0036 ACCEPT 101,ANSA
0037 IF (ANSA.NE.'Y') GO TO 111
0038 TYPE *, ' Enter Min area (Sq. pix) and Scale (mm/pix)'
0039 ACCEPT *,ARMIN,SCALE
0040 GO TO 111
0041 900 TYPE *, ' File has already data, Stops execution (Y/N)?'
0042 ACCEPT 101,ANSA
0043 IF (ANSA.EQ.'Y') GO TO 950
C
C First detector
C
0044 111 TYPE *, ' Begin coarse detection'

FORTRAN IV-N 3 V02-51 10:50:17 26-APR-85
DROPS.FTN

1 2

0045 CALL SETUP
0046 TYPE *, ' Smoothing before compute gradient (Y/N)'
0047 ACCEPT 101,ANSA
0048 IF (ANSA.EQ.'N') GO TO 4
0049 CALL SMOOTH
0050 GO TO 5
0051 4 DO 3 K=1,256
0052 3 (VLT(K)=K/2
0053 CALL VLTCUR(1,IVLT)
C
C Save original picture
C
0054 5 CALL SETUP
0055 OPEN (UNIT=7,TYPE='SCRATCH',ACCESS='DIRECT',INITIALSIZE=512,
IRECORDSIZE=120)
NBLK=1
0056 DO 10 K=1,32
0057 LIN=(K-1)*16+1
0058 ICOD=IMAGE(8,LIN,16,'R',PIXEL)
0059 ISTAT=JESC(7,PIXEL,NBLK,4096,1,NBLK)
0060 CONTINUE
C
C Transfer smooth picture to channel 8
C
0062 CALL SETUP
0063 CALL INSEL(2,8,8)
0064 CALL OUTBL(1)
0065 CALL FMOPER
C
C Compute gradient
C
0066 CALL SETUP
0067 CALL GRADIE
C
C Restore original picture
C
0068 CALL SETUP
NBLK=1
0069 DO 20 K=1,32
0070 LIN=(K-1)*16+1
0071 ISTAT=JEEC(7,PIXEL,NBLK,4096,1,NBLK)
0072 ICOD=IMAGE(8,LIN,16,'W',PIXEL)
0073 CONTINUE
C
C Threshold gradient picture
C
0075 CALL SETUP
0076 CALL INSEL(1,8,8)
0077 CALL OUTBL(4)
0078 CALL FMOPER
0079 CALL SETUP
0080 50 TYPE *, ' Threshold gradient Image', ICORTA
0081 CALL SETUP
0082 DO 51 JLT=1,ICORTA
0083 51 IVLT(JLT)=JLT
0084 DO 52 JLT=ICORTA+1,256

FORTRAN IV-
 DROPS.FTH S V02-51 10:50:17 26-APR-05 E 3
 0085 52 IVLT(JLT)=255
 0086 CALL VIDTHRK(1,IVLT)
 0087 TYPE *,' Accept threshold (y/n)'
 0088 ACCEPT 101,AHSA
 0089 IF (AHSA.NE.'N') GO TO 68
 0090 TYPE *,' Enter gradient image threshold'
 0091 ACCEPT *,ICORTA
 0092 GO TO 50
 0093 101 FORMAT(A1)
 0094 68 CALL SETUP
 0095 DO 70 JLT=ICORTA+1,256
 0096 70 IVLT(JLT)=JLT-1
 0097 CALL VLTCK(1,IVLT)
 0098 CALL SETUP
 C
 C Save gradient picture
 C
 NBLK=1
 DO 80 K=1,32
 LTH=(K-1)*16+1
 ICOD=IMAGE(1,LIN,16,'R',PIXEL)
 ISTAT=JESC(7,PIXEL,NBLK,4096,1,NBLK)
 0104 80 CONTINUE
 C
 Remove background variations
 C
 TYPE *,' Remove background variations (Y/N)'
 ACCEPT 101,AHSD
 IF (AHSD.NE.'N') GO TO 85
 CALL INSEL(2,B,B)
 CALL OUTNBL(4)
 CALL FPROPER
 CALL SETUP
 CALL INSEL(1,B,B)
 CALL OUTNBL(2)
 CALL FPROPER
 CALL SETUP
 GO TO 80
 0117 85 ISO=100 ! Variations scale
 CALL HIGHPASS(ISO,1,B)
 CALL SETUP
 C
 Restore gradient picture
 C
 NBLK=1
 DO 120 K=1,32
 LTH=(K-1)*16+1
 ISTAT=JLEEC(7,PIXEL,NBLK,4096,1,NBLK)
 ICOD=IMAGE(2,LIN,16,'W',PIXEL)
 0125 120 CONTINUE
 C
 Compute Histogram
 C
 0126 80 ZERO=*0
 TYPE *,' Computing modified PDF'
 DO 90 K=0,255

```
0129      90      HIST(K)=0.  
0130      DO 150 K=10,500  
0131      ICOD=IMAGE(1,K,1,'R',BUGIC)  
0132      ICOD=IMAGE(2,K,1,'R',BUGRA)  
0133      DO 150 J=10,500  
0134      IF (BUGRA(J),EQ,ZERO) GO TO 150  
0135      A=IV(BUGRA(J))  
0136      II=IV(BUPIC(J))  
0137      HIST(II)=HIST(II)+II*A  
0138      150      CONTINUE  
C  
C      Display histogram and threshold determination  
C  
0139      DMAXO=0.  
0140      DO 180 K=0,255  
0141      IF (HIST(K),GT,DMAXO) DMAXO=HIST(K)  
0142      180      CONTINUE  
0143      DO 182 K=0,255  
0144      HIST(K)=HIST(K)/DMAXO  
0145      182      CONTINUE  
0146      CALL INSEL(1,0,0)  
0147      CALL OUTNBL(4)  
0148      CALL FMOPER  
0149      CALL SETUP  
0150      DO 160 K=1,256  
0151      IVLT(K)=0  
0152      CALL VIDTHR(1,IVLT)  
0153      ITHR=0  
0154      CALL DIGHIS(HIST,ITHR)  
0155      TYPE *, ' Enter (1) simple, (2) bimodal distribution'  
0156      ACCEPT *,INODES  
0157      CALL SEUDSO(HIST,ITHR,INODES)  
0158      300      TYPE *, ' Estimated threshold',ITHR  
0159      CALL SETUP  
0160      DO 391 JLT=1,ITHR  
0161      IVLT(JLT)=0  
0162      DO 392 JLT=ITHR+1,256  
0163      IVLT(JLT)=255  
0164      CALL VI(TCOR(1,IVLT)  
0165      CALL SETUP  
0166      IVLT(1)=0  
0167      IVLT(256)=1  
0168      CALL VI(TCOR(1,IVLT)  
0169      CALL SETUP  
0170      CALL BORDEAK(IVLT)  
0171      CALL SETUP  
0172      CALL DIGHIS(HIST,ITHR)  
0173      TYPE *, ' Accept threshold (Y/N)?'  
0174      ACCEPT 101,ANS1  
0175      IF (ANS1,NE,'N') GO TO 350  
0176      TYPE *, ' Enter threshold'  
0177      ACCEPT *,ITHR  
0178      IF (ANS1,NE,'N') GO TO 320  
0179      CALL INSEL(1,0,0)  
0180      CALL OUTNBL(2)  
0181      CALL FMOPER
```

```

0102      CALL SETUP
0103      GO TO 300
0104      320      CALL RIGPAS(ISO,1,0)
0105      CALL SETUP
0106      GO TO 300
0107      350      TYPE *, ' Default region the entire picture change (Y/N)'
0108      ACCEPT IO1,ANS1
0109      IF (ANS1.EQ.'Y') GO TO 400
0110      SL=1
0111      SS=1
0112      NL=510
0113      NS=510
0114      GO TO 450
0115      400      TYPE *, ' Use cursor to define region/push white key'
0116      CALL REGIO(SL,SS,NL,NS)
0117      C
0118      450      ARINAR=ARINR
0119      TYPE *, ' Region definition SL=',SL,' SS=',SS,' NL=',NL,' NS=',NS
0120      IVLT(1)=0
0121      IVLT(2)=255
0122      IVLT(256)=255
0123      CALL VLTCOR(1,IVLT)
0124      CALL SETUP
0125      TYPE *, ' Computing drops size'
0126      CALL GOTAG(1,SL,SS,NL,NS,ABUF,PBUF,LIMIT,NUMOBJ)
0127      IVLT(1)=0
0128      IVLT(256)=1
0129      CALL VLTCOR(1,IVLT)
0130      CALL BORDEA(IVLT)
0131      CALL SETUP
0132      TYPE *, ' End coarse detector'
0133      CLOSE(UNIT=7)
0134      C
0135      C      Save results on disk
0136      C
0213      2000      HUMDR=0
0214      SCALER=SCALE*SCALE
0215      TYPE *, ' DATABASE: Initial element',KREDC
0216      DO 2001 K=1,NUMOBJ
0217      HUMDR=HUMDR+1
0218      KREDC=KREDC+1
0219      PL=LINIT(1,K)
0220      PR=LINIT(2,K)
0221      PC=LINIT(3,K)
0222      CL=LINIT(4,K)
0223      AREA=ABUF(K)*SCALE2
0224      PERIM=PBUF(K)*SCALE
0225      WRITE(7)KREDC,1B0FE
0226      IF (KREDC.EQ.1281) GO TO 2025
0227      CONTINUE
0228      2001      TYPE *, ' DATABASE: Final element',KREDC-1
0229      TYPE *, ' Number of objects in this frame',NUMDR
0230      WRITE(7)1B0FU1Update general information record
0231      950      CLOSE(UNIT=3)
0232      END

```

FORTRAN, IV-PL V92-51 14:09:02 25-APR-85 PA 1
 GOTAS.FTN /TR:BLOCKS/VR

```

0001      SUBROUTINE GOTAS(CHAN,SL,SS,NL,NS,ABUF,PBUF,LIMIT,NUMOBJ)
C
C   Drops geometrical characterization
C
0002     INTEGER*2 CHAN,SL,SS,NL,NS
0003     BYTE PIXEL(512,16)
0004     COMMON /PINTA/PIXEL
0005     INTEGER*2 FLAG(512,2),ID(38)
0006     INTEGER*2 ISLG(98),ISGS(98),EL(98),ES(98)
0007     INTEGER*2 CNTR(98,2),BEGIN(98,2),END(98,2)
0008     INTEGER*2 OLDID,NEWID
0009     INTEGER*4 NPIXG(98)
0010     REAL*4 RPER(98)
0011     REAL*4 ABUF(1),PBUF(1)
0012     INTEGER*2 LIMIT(4,1)

C   Initialize
C
0013     CALL ZIAFLAG(1,1),1024)
0014     CALL ZIACRPER,100)
0015     CALL ZIACNPIXS,100)
0016     CALL ZIACEL,98)
0017     CALL ZIACES,98)
0018     CALL ZIACCTR(1,1),100)
0019     CALL ZIACBEGIN(1,1),100)
0020     CALL ZIACEND(1,1),100)
0021     CALL ITIAC32000,ISLS,98)
0022     CALL ITIAC32000,ISGS,98)
0023     NUMOBJ=0
0024     LSV=1
0025     NWYC=0
0026     HOC=0
0027     OLDID=1
0028     NSG=SS+NG
0029     HSL=SL-1
0030     HLL=HSL+NU

C   Main loop
C
0031     DO 100 L=1,NL,16
0032       LBLOCK=MIN(16,NL-L)
0033       LINE=L+HSL
0034       ICOD=IMAGE(CHAN,LINE,1BLOCK,'R',PIXEL)
0035       DO 100 KK=1,16
0036         K1=SS
0037         LTHIA=LINE+KK-1
0038         NWYC=0 ! Start searching for an object at 0
0039         DO 110 J=K1,NSG ! Look for left edge
0040           IF (.PTREL(J,KK)) GO TO 120
0041         110    CONTINUE
0042         C      No more edges on this line
0043         GO TO 103
0044         120    H1=J ! Left edge
0045         DO 130 J=H1,NSG ! Look right edge
0046           IF (.PTREL(J,KK)) GO TO 140
0047         130    CONTINUE
  
```

FORTRAN IV-PL V02-51 14:09:02 25-APR-85 PA 12
 GOTAS.FTN TR:BLOCKS/WR

```

0047      J=NSS+1 ! Right edge is the picture boundary
0048      140
0049      C
0050      C      Find ID of this object from previous flag line
0051      C
0052      C      CALL MATCH(FLAG(1,3-ISW),N1,N2,NUM,ID,NSS)
0053      C      NEWID=ID(1)
0054      C      IF (NUM.LT.2) GO TO 181
0055      C      C      If many ID condense them into one
0056      C      CALL COND(RPER,NPIXS,ISLS,ISSS,EL,ES,NUM,ID)
0057      C      GO TO 182
0058      C      IF (NUM.NE.0) GO TO 182
0059      C      C      If there is not ID then creates one
0060      C      CALL FIND(90,NEWID,NPIXS,OLDID)
0061      C      C      begin counting perimeter new object
0062      C      RPER(NEWID)=N2-N1+2
0063      C      C      And update flag buffer and counters
0064      C      CALL ITIA(NEWID,FLAG(N1,ISW),N2-N1+1)
0065      C      NEWC=NEWC+1
0066      C      CNTR(NEWC,ISW)=NEWID
0067      C      BEGIN(NEWC,ISW)=N1
0068      C      IEND(NEWC,ISW)=N2
0069      C      C      Update statistics buffer
0070      C      RPIXS(NEWID)=RPIXS(NEWID)+N2-N1+1
0071      C      IF ((ISLS(NEWID)).GT.LINIA) ISLS(NEWID)=LINIA
0072      C      IF ((ISSS(NEWID)).GT.N1) ISSS(NEWID)=N1
0073      C      IF ((ES(NEWID)).LT.N2) ES(NEWID)=N2
0074      C      EL(NEWID)=LINIA
0075      C      CALL PERIM(HOLC,NEWC,CNTR(1,ISW),NEWID,RPER,BEGIN(1,3-ISW),
0076      C      1 BEGIN(1,ISW),IEND(1,3-ISW),IEND(1,ISW))
0077      C      C      Send back for more data on the same line
0078      C      N1=N2+2
0079      C      IF (N1.LE.NSS) GO TO 185
0080      C      C      Search buffers for terminated drops
0081      C      103
0082      C      CALL ENDFL(RPER,NPIXS,ISLS,ISSS,EL,ES,NLL,LINIA,CNTR(1,3-ISW),
0083      C      1     CNTR(1,ISW),NOLC,NEWC,NUMOBJ,BEGIN(1,3-ISW),BEGIN(1,ISW),
0084      C      2     IEND(1,3-ISW),IEND(1,ISW),ABUF,PBUF,LIMIT)
0085      C      CALL ZIA(FLAG(1,3-ISW),512) ! Zero flag line
0086      C      ISW=3-ISW ! Switch the flag
0087      C      NOLC=NEWC
0088      C      CONTINUE ! Close main loop
0089      C      RETURN
0090      C      END
  
```

FORTRAN IV-F
MATCH.FTN

V92-51
/TR:BLOCKS/WR

19:01:38

84-APR-85

P 1

```
0001      SUBROUTINE MATCH(FLAG,N1,N2,NUM, ID,NS)
C
C      RETURN I.D. OF OBJECT FOUND ON PREVIOUS LINE
C      FLAG = OLD FLAG BUFFER
C      N1 = BEGIN, N2 = END OF OBJECT
C      NUM = NUMBER OF OBJECTS LOCATED
C      ID = I.D. OF OBJECTS LOCATED
0002      INTEGER FLAG(1)
0003      INTEGER*4 ID(1)
0004      M1 = N1 - 1
0005      M2 = N2 + 1
0006      IF (M1.LT.1) M1 = 1
0007      IF (M2.GT.NS) M2=NS
0008      NUM = 0
0009      K = 0
C
C      FIND ALL FLAGS
C
0010      DO 10 J=M1,M2
0011      IF (FLAG(J).EQ.K) GO TO 10
0012      IF (FLAG(J).EQ.0) GO TO 10
0013      K = FLAG(J)
0014      NUM = NUM + 1
0015      ID(NUM) = K
0016      10    CONTINUE
0017      IF (NUM.LT.2) RETURN
C
C      REJECT DUPLICATES
C
0018      CALL CORSRT(ID, ID,NUM)
0019      N = 1
0020      K = ID(1)
0021      DO 20 J=2,NUM
0022      IF (K.EQ.ID(J)) GO TO 20
0023      N = N + 1
0024      ID(N) = ID(J)
0025      20    CONTINUE
0026      NUM = N
0027      RETURN
0028      END
```

FORTRAN IV-F V82-51 19:01:84 84-APR-86 P 1
 PERJM.FTN /TR:BLOCKS/WR

```

0001      SUBROUTINE PERIM(NOLC,NEWC,NECNTR,NEWID,RPER,OBEGIN,NBEGIN,
1          OEND,NEND)
C
C      THIS SUBROUTINE ACCUMULATES PERIMETER MEASUREMENTS FOR THE 'OLD'
C      LINE BETWEEN N1 AND N2 OF THE 'NEW' LINE.
C
0002      INTEGER NECNTR(1),OBEGIN(1),NBEGIN(1),OEND(1),NEND(1)
0003      REAL*4 RPER(1)
0004      IF (NOLC.EQ.0) RETURN
C
C      SEARCH 'OLD' LINE FOR MATCHING OBJECT SEGMENTS.
C
0005      L1 = 0
0006      DO 100 J=1,NOLC
0007      IF (OEND(J).GE.NBEGIN(NEWC)-1.AND.
1          OBEGIN(J).LE.NEND(NEWC)+1) GO TO 101
0008      GO TO 100
0009      101  ONEWC = NEWC - 1
0010      IF (ONEWC.LT.1) GO TO 301
0011      IF (NEWID.EQ.NECNTR(ONEWC).AND.OEND(L2).GE.NBEGIN(NEWC))
1          GO TO 302
0012      GO TO 301
C
C      IF PERIMETER HAS BEEN ADDED FOR PREVIOUS PARTICLE SEGMENT ON
C      'NEW' LINE WITH SAME I.D. AND THE 'OLD' MATCHING SEGMENT
C      OVERLAPS BOTH 'NEW' SEGMENTS, THEN THE OVERLAP IN THE
C      CURRENT SEGMENT IS SUBTRACTED FROM THE PERIMETER VALUE.
C
0013      302  RPER(NEWID) = RPER(NEWID) - SQRT((OEND(L2)
1          - FLOAT(NEND(ONEWC)))**2 + 1.) + NBEGIN(NEWC) - NEND(ONEWC)
0014      GO TO 303
0015      301  RPER(NEWID) = RPER(NEWID) + SQRT((NBEGIN(NEWC)
1          - FLOAT(OBEGIN(J)))**2 + 1.)
0016      303  L1 = J
0017      K = J + 1
0018      GO TO 102
0019      100  CONTINUE
0020      102  IF (L1.EQ.0) RETURN
0021      L2 = 0
0022      IF (K.GT.NOLC) GO TO 200
0023      DO 103 J=K,NOLC
0024      IF (OEND(J).GE.NBEGIN(NEWC)-1.AND.
1          OBEGIN(J).LE.NEND(NEWC)+1) GO TO 104
0025      GO TO 103
0026      104  RPER(NEWID) = RPER(NEWID) + (OBEGIN(J) - OEND(J-1))
0027      L2 = J
0028      103  CONTINUE
0029      200  IF (L2.EQ.0) L2 = L1
0030      RPER(NEWID) = RPER(NEWID) + SQRT((NEND(NEWC)
1          - FLOAT(OEND(L2)))**2 + 1.)
0031      RETURN
0032      END
  
```

FORTRAN IV-
CONID.FTN

S V82-51
/TR:BLOCKS/WR

18:59:52

84-APR-85

: 1

8881 SUBROUTINE CONID(RPER,NPIXS,ISLS,ISSS,EL,ES,NUM, ID)
C
C USED TO CONCATINATE MANY I.D.'S
C
8882 INTEGER OLDID,ISLS(1),ISSS(1),EL(1),ES(1)
8883 INTEGER*4 NPIXS(1),ID(1)
8884 REAL*4 RPER(1)
8885 NEWID = ID(1)
8886 DO 10 J=2,NUM
8887 OLDID = ID(J)
8888 RPER(NEWID) = RPER(NEWID) + RPER(OLDID).
8889 RPER(OLDID) = 0.
8810 NPIXS(NEWID) = NPIXS(NEWID) + NPIXS(OLDID)
8811 NPIXS(OLDID) = 0
8812 IF (ISLS(NEWID).GT.ISLS(OLDID)) ISLS(NEWID) = ISLS(OLDID)
8813 ISLS(OLDID) = 32000
8814 IF (ISSS(NEWID).GT.ISSS(OLDID)) ISSS(NEWID) = ISSS(OLDID)
8815 ISSS(OLDID) = 32000
8816 IF (EL(NEWID).LT.EL(OLDID)) EL(NEWID) = EL(OLDID)
8817 EL(OLDID) = 0
8818 IF (ES(NEWID).LT.ES(OLDID)) ES(NEWID) = ES(OLDID)
8819 ES(OLDID) = 0
8820 RETURN
8821 END

FORTRAN IV-P V82-51 19:02:52 84-APR-85 P 1
PCNCAT.FTN /TR:BLOCKS/WR

0001 SUBROUTINE PCNCAT(NCEN,PCNTR,BEGIN,END,NEWID,RPER)
C THIS SUBROUTINE CONCATINATES ALL ENDING PERIMETER VALUES FOR EACH
C I.D. ON AN ENDING LINE.
C
0002 INTEGER PCNTR(1),BEGIN(1),END(1)
0003 REAL*4 RPER(1)
0004 DO 100 J=1,NCEN
0005 IF (NEWID.EQ.PCNTR(J)) GO TO 101
0006 GO TO 100
0007 101 RPER(NEWID) = RPER(NEWID) + END(J) - BEGIN(J) + 2.
0008 100 CONTINUE
0009 RETURN
0010 END

FORTRAN IV-F
FIND.FTM

V82-51
/TR:BLOCKS/WR

19:03:00 84-APR-85

P 1

8881 SUBROUTINE FIND(NBIN,NEWID,NPIXS,OLDID)
C
C USED TO FIND A NEW BIN POSITION
C NBIN = LENGTH OF BIN BUFFERS
C NEWID = NEW BIN VALUE RETURNED
C NPIXS = SUM OF PIXELS BUFFER
C OLDID = LAST FOUND I.D.
8882 INTEGER OLDID
8883 INTEGER*4 NPIXS(1)
8884 DO 100 J=OLDID,NBIN
8885 IF (NPIXS(J).EQ.0) GO TO 200
8886 CONTINUE
8887 DO 150 J=1,OLDID
8888 IF (NPIXS(J).EQ.0) GO TO 200
8889 CONTINUE
8890 TYPE *, ' All bins filled'
8891 STOP
8892 NEWID=J
8893 OLDID=J
8894 RETURN
8895 END

FORTRAN IV-P
CORSRT.FTN

V82-51
/TR:BLOCKS/WR

19:03:28 84-APR-85

P 1

0001 SUBROUTINE CORSRT(KEY,PTR,LEN)

C IN CORE SORT ROUTINE. SORTS THE VECTORS KEY AND PTR INTO ASCENDING ORDER OF
C KEY. THE VALUES IN KEY ARE TREATED AS LOGICAL QUANTITIES HENCE SIGN BITS
C MUST BE TREATED ACCORDINGLY. ALPHABETIC RECORDS MAY BE SORTED SINCE
C CHARACTER CODES ARE IN LOGICAL ORDER. THE PTR ARRAY CAN THEN BE USED TO MOV
C RECORDS IN A DISK FILE.

C
0002 IMPLICIT INTEGER(A-Z)
0003 INTEGER*4 IMSK,JMSK,SM(32),PTR(1),TEMP
0004 LOGICAL*4 IMSL,JMSL,KEY(1),LTEMP
0005 DIMENSION BDRY(3,32),CBD(32)
0006 EQUIVALENCE (IMSK,IMSL),(JMSK,JMSL)
0007 DATA SM(1),SM(2),SM(17)/020000000000,010000000000,01000000/
C
0009 DO 1 I=3,16
0010 1 SM(1) = SM(I-1)/2
0011 DO 2 I=10,32
0012 2 SM(1) = SM(I-1)/2
0013 LEV = 1
0014 BDRY(2,LEV) = 1
0015 BDRY(3,LEV) = LEN
0016 CBD(LEV) = 2
0017 72 CB = CBD(LEV)
0018 PL = BDRY(CB,LEV)
0019 PU = BDRY(CB+1,LEV)
0020 IF (PL.GE.PU) GO TO 75
0021 IMSK = SM(LEV)
0022 JMSL = KEY(PL).AND. IMSL
0023 IF (JMSK.NE.0) GO TO 85
0024 PL = PL + 1
0025 IF (PL.EQ.PU) GO TO 73
0026 GO TO 81
0027 85 JMSL = KEY(PU).AND. IMSL
0028 IF (JMSK.NE.0) GO TO 86
0029 LTEMP = KEY(PL)
0030 TEMP = PTR(PL)
0031 KEY(PL) = KEY(PU)
0032 PTR(PL) = PTR(PU)
0033 KEY(PU) = LTEMP
0034 PTR(PU) = TEMP
0035 GO TO 81
0036 86 PU = PU - 1
0037 IF (PU.NE.PL) GO TO 85
0038 JMSL = KEY(PL).AND. IMSL
0039 IF (JMSK.NE.0) PL = PL - 1
0040 IF (LEV.GE.32) GO TO 75
0041 CB = CBD(LEV)
0042 LEV = LEV + 1
0043 CBD(LEV) = 1
0044 BDRY(1,LEV) = BDRY(CB,LEV-1)
0045 BDRY(2,LEV) = PL
0046 BDRY(3,LEV) = BDRY(CB+1,LEV-1)
0047 GO TO 72
0048 75 IF (CBD(LEV).EQ.2) GO TO 76
0049 CBD(LEV) = 2

FORTRAN-IV-P V82-51 19:03:28 84-APR-85 P 2
CORSRT.FTN /TR:BLOCKS/VR

0049 BDRY(2,LEV) = BDRY(2,LEV) + 1
0050 GO TO 72
0051 76 LEV = LEV - 1
0052 IF (LEV.GT.0) GO TO 75
0053 RETURN
0054 END

FORTRAN-IV-P V82-51 19:01:54 84-APR-85 P 1
 ENOFLI.FTN,
 /TR:BLOCKS/WR

```

0001      SUBROUTINE ENOFLI(RPER,NPIXS,ISLS,ISSS,EL,ES,NL,LINE,
1      OLCNTR,NECNTR,NOLC,NEWC,NUM,UBEGIN,NBEGIN,
2      OEND,MEND,ABUF,PBUF,LIMIT)

C      SEARCH FOR FINISHED OBJECTS
C
0002      INTEGER*4 NPIXS(1)
0003      INTEGER OLCNTR(1),NECNTR(1),OBEGIN(1),NBEGIN(1),OEND(1),MEND(1)
0004      INTEGER ISLS(1),ISSS(1),EL(1),ES(1)
0005      REAL*4 RPER(1),ABUF(1),PBUF(1)
0006      INTEGER*2 LIMIT(4,1)

C      SEARCH OLCNTR FOR I.D.'S NOT IN NECNTR
C
0007      IF (LINE.EQ.NL) GO TO 52
0008      IF (NOLC.EQ.0) RETURN
0009      IF (NEWC.EQ.0) GO TO 51
0010      DO 10 J=1,NOLC
0011      NEWID = OLCNTR(J)
0012      DO 20 K=1,NEWC
0013      IF (NEWID.EQ.NECNTR(K)) GO TO 18
0014      20  CONTINUE
C      DROPLET NOT CONTINUED
C
0015      CALL PCNCAT(NOLC,OLCNTR,OBEGIN,OEND,NEWID,RPER)
0016      CALL FINAL(NEWID,RPER,NPIXS,ISLS,ISSS,EL,ES,NUM,ABUF,
1      PBUF,LIMIT)
0017      18  CONTINUE
0018      RETURN
C      FINISH OFF EVERYTHING
C
0019      51  DO 50 J=1,NOLC
0020      NEWID = OLCNTR(J)
0021      CALL PCNCAT(NOLC,OLCNTR,OBEGIN,OEND,NEWID,RPER)
0022      CALL FINAL(NEWID,RPER,NPIXS,ISLS,ISSS,EL,ES,NUM,ABUF,
1      PBUF,LIMIT)
0023      50  CONTINUE
0024      RETURN
0025      52  IF (NOLC.EQ.0) GO TO 60
0026      IF (NEWC.EQ.0) GO TO 51
0027      DO 80 J=1,NOLC
0028      NEWID = OLCNTR(J)
0029      DO 90 K=1,NEWC
0030      IF (NEWID.EQ.NECNTR(K)) GO TO 100
0031      90  CONTINUE
0032      CALL PCNCAT(NOLC,OLCNTR,OBEGIN,OEND,NEWID,RPER)
0033      CALL FINAL(NEWID,RPER,NPIXS,ISLS,ISSS,EL,ES,NUM,ABUF,
1      PBUF,LIMIT)
0034      GO TO 80
0035      100  CALL PCNCAT(NEWC,NECNTR,NBEGIN,MEND,NEWID,RPER)
0036      CALL FINAL(NEWID,RPER,NPIXS,ISLS,ISSS,EL,ES,NUM,ABUF,
1      PBUF,LIMIT)
0037      80  CONTINUE
0038      RETURN
  
```

FORTRAN-IV-P
ENOFI1.FTN

V82-51
/TR:BLOCKS/WR

19:51:54

84-APR-85

P 2

```
0039      68 IF (NEWC.EQ.0) RETURN
0040      DO 70 J=1,NEWC
0041      NEWID = NECNTR(J)
0042      CALL PCNCAT(NEWC,NECNTR,NBEGIN,NEND,NEWID,RPER)
0043      CALL FINAL(NEWID,RPER,NPIXS,ISLS,ISSS,EL,ES,HUM,ABUF,
1          PBUF,LIMIT)
0044      70 CONTINUE
0045      RETURN
0046      END
```

```
0001      SUBROUTINE FINAL(NEWID,RPER,NPIXS,ISLS,ISSS,EL,ES,NUM,ABUF,
          1           PBUF,LIMIT)
C
C   TO TERMINATE AN OBJECT
C
0002      INTEGER*4 NPIXS()
0003      INTEGER*2 LIMIT(4,1)
0004      INTEGER ISLS(1),ISSS(1),EL(1),ES(1)
0005      REAL*4 RPER(1),ABUF(1),PBUF(1)
0006      BYTE ORIGA(512)
0007      COMMON /MINARE/ AMINAR
0008      IF (NPIXS(NEWID).EQ.0) RETURN
0009      NUM = NUM + 1
0010      IF (NUM.LT.2) GO TO 5
0011      TYPE *, ' Number of spots gt buffer space available'
0012      STOP
C
C   ACCUMULATE DROPLET STATISTICS
C
0013      5      ABUF(NUM) = NPIXS(NEWID)
0014      PBUF(NUM) = RPER(NEWID)
0015      LIMIT(1,NUM) = ISLS(NEWID)
0016      LIMIT(2,NUM) = ISSS(NEWID)
0017      LIMIT(3,NUM) = EL(NEWID) - ISLS(NEWID) + 1
0018      LIMIT(4,NUM) = ES(NEWID) - ISSS(NEWID) + 1
C   CLEAR OUT BINS
0019      IF (ABUF(NUM).GT.AMINAR) GO TO 10
0020      CALL BORRAR(1,LIMIT(1,NUM),LIMIT(2,NUM),LIMIT(3,NUM),LIMIT(4,NUM))
0021      NUM=NUM-1
C
0022      10      NPIXS(NEWID) = 0
0023      RPER(NEWID) = 0.
0024      ISLS(NEWID) = 32000
0025      ISSS(NEWID) = 32000
0026      EL(NEWID) = 0
0027      ES(NEWID) = 0
0028      RETURN
0029      END
```

APPENDIX B
DROPLET STATISTICS PROGRAM

FORTRAN IV-P
RAINST.FTN

V82-51
/TR:BLOCKS/WR

10:58:38 23-FEB-84

P 1

0001

PROGRAM RAINST

C

Read droplets' data file and compute general statistic

C

Programmer: Miguel A. Hernan

C

```
REAL*4 DBUF(1200),VOLUME(1200),ESFER(1200)
REAL*8 SHD1,SHD2,DTOT,ESTOT,SHD4,COMOD
INTEGER*2 NHUE
LOGICAL*1 ANSA
REAL*4 VOLHIS(0:79),FREHIS(0:79)
REAL*4 AREA,PERIM,D3,D2,D,DA
LOGICAL*1 NOZODC(12),NOZIN(68),NOZID(88)
EQUIVALENCE(NOZODC(1),NOZID(1))
EQUIVALENCE(NOZIN(1),NOZID(13))
INTEGER*2 OPEPIO
LOGICAL*1 FILEAC(22)
INTEGER*2 IBUFER(0),SL,SG,ML,NS
EQUIVALENCE(IBUFER(1),SL)
EQUIVALENCE(IBUFER(2),SG)
EQUIVALENCE(IBUFER(3),ML)
EQUIVALENCE(IBUFER(4),NS)
EQUIVALENCE(IBUFER(5),AREA)
EQUIVALENCE(IBUFER(7),PERIM)
DATA VOLHIS/0/,*/,FREHIS/0/,*/,/
DATA NOZOD /'N','O','Z','Z','L','E','I','I','D','I','I','I,'/
```

C

Open data file

FORHAT(0,22A1)

TYPE *, ' Enter filename'

ACCEPT 451,LONGU,(FILENA(I),I=1,LONGO)

C

```
OPEN(UNIT=3,NAME=FILENA,TYPE='OLD',
      IOSTAT='KEEP',ACCESS='DIRECT',RECORDSIZE=4,FORM='UNFORMATTED')
READ(3(K)) IBUFER
NHUE=IBUFER(1)
ICONT=0
SHD4=0.
SHD3=0.
SHD2=0.
DTOT=0.
ESTOT=0.
PI=3.14159
Q1=4./(3.*SQRT(PI))
```

C

Main loop

DO 100 K=2,NHUE

READ(3(K)) IBUFER

IF (IBUFER(1).EQ.0) GO TO 200

ICONT=ICONT+1

D2=(4.*AREA)/PI

D=SQRT(D2)

D1=D/2**0

D4=D/2**02

ESFER(ICONT)=(PERIM*PERIM)/(AREA*4.*PI)

DBUF(ICONT)=0

FORTRAN IV-P
 RAINST.FTM V02-51 10:58:30 23-FEB-84 P 2
 /TR:BLOCKS/VR

```

0046      VOBUF(ICONT)=Q1*(AREA**1.5)
0047      SHD4=SHD4+D4
0048      SHD3=SHD3+D3
0049      SHD2=SHD2+D2
0050      DTOT=DTOT+D
0051      ESTOT=ESTOT+ESFER(ICONT)
11=19*0
11=HINR(79,11)
0053      FREHIS(11)=FREHIS(11)+1
0054      VOLHIS(11)=VOLHIS(11)+D3
0055      100  CONTINUE
0056      CLOSE(UNIT=3)
0057      GO TO 300
0058      200  CLOSE(UNIT=3)
0059      TYPE *, ' File records counter error'
0060      CALL EXIT
C
C          Begin general statistic
C
0062      300  TYPE *, ' Enter nozzle code'
0063      ACCEPT 75H,1TEX,(NOZIN(1),I=1,1TEX)
0064      75H  FORMAT(2,6A1)
0065      TYPE *, ' Enter water pressure (psi)'
0066      ACCEPT 5,WATP
0067      TYPE *, ' Enter wind tunnel speed (ft/sec)'
0068      ACCEPT 6,WTS
0069      TYPE *, ' Enter downstream coordinate (inch)'
0070      ACCEPT 7,DOWL
0071      PRINT 4,NOZOD,(NOZIN(1),I=1,1TEX)
0072      PRINT 5,WATP
0073      PRINT 6,WTS
0074      PRINT 7,DOWL
0075      PRINT 11,ICONT
0076      4   FORMAT(X,12A1,6A1)
0077      5   FORMAT(' Water pressure =',F6.2,' psi')
0078      6   FORMAT(' Wind tunnel speed =',F6.2,' ft/sec')
0079      7   FORMAT(' Downstream location =',F6.2,' inch')
0080      11  FORMAT(' Number of Drops =',I5)
0081      PRINT 12
0082      12  FORMAT(' Length diameter (D10)=')
0083      NAMO=ICONT
0084      CALL STAT(NAMO,DBUF,DTOT)
0085      PRINT 13,SQRT(SHD2/FLOAT(ICONT))
0086      13  FORMAT(' Area mean diameter (D20)=' ,F15.6)
0087      COMOD=SHD3*PI/6.
0088      PRINT 17,COMOD
0089      17  FORMAT(' Drops total volume=' ,F15.6)
0090      NAMO=ICONT
0091      CALL STAT(NAMO,VOBUF,COMOD)
0092      VOLMED=SHD3/FLOAT(ICONT)
0093      VOLMED=VOLMED**(.1/3.)
0094      PRINT 14,VOLMED
0095      14  FORMAT(' Volume mean diameter (D30)=' ,F15.6)
0096      PRINT 15,SHD3/SHD2
0097      16  FORMAT(' Sauter mean diameter (D32)=' ,F15.6)
0098      PRINT 30,SHD4/SHD3
  
```

FORTRAN IV-P
 RAINST.FTM V02-51 10:59:30 23-FEB-84 P 3
 /TR:BLOCKS/WR

```

0100      30      FORMAT(' Volume distribution mean diameter (D43)=',F15.6)
0101      PRINT 31
0102      31      FORMAT(' Circularity (perimeter**2/area*4pi)')
NAMO=ICONT
0103      CALL STATS(NAMO,ESPER,ESTOT)
0104      TYPE *, ' Plot the distributions (Y/N)'
0105      ACCEPT 800,ANSA
0106      800      FORMAT(A1)
0107      IF (ANSA.NE.'Y') GO TO 800
0108      OPEPLO=0
0109      SAMP=FLOAT(ICONT)/100.
0110      SHD3=SHD3/100.
0111      DO 500 K=0,.79
0112      VOLHIS(K)=VOLHIS(K)/SHD3
0113      FREHIS(K)=FREHIS(K)/SAMP
CONTINUE
0115      TYPE *, ' Frequency distribution (Y/N)'
0116      ACCEPT 800,ANSA
0117      IF (ANSA.NE.'Y') GO TO 600
0118      CALL RAINHI(FREHIS,OPEPLO,0.,.1)
0119      IF (OPEPLO.EQ.0) GO TO 600
0120      OPEPLO=OPEPLO
0121      CALL SYMBOL(-4.3,1.15,.1,'DROPS DIAMETER FREQUENCY DISTRIBUTION',
0122           ' 00.,.37)
0123      CALL SYMBOL(-1.35,-.75,.1,'FREQUENCY (%)',100.,.13)
0124      GO TO 400
0125      600      TYPE *, ' Cumulative volume distribution (Y/N)'
0126      ACCEPT 800,ANSA
0127      IF (ANSA.NE.'Y') GO TO 650
0128      CALL RAINHI(VOLHIS,OPEPLO,0.,.1)
0129      IF (OPEPLO.GE.0) GO TO 650
0130      CALL SYMBOL(-4.3,1.45,.1,'VOLUME CONTRIBUTION VS DIAMETER',90.,.31)
0131      CALL SYMBOL(-.05,-.75,.1,'VOLUME CONTRIBUTION (%)',100.,.23)
0132      400      CALL SYMBOL(-7.2,35,.1,'DIAMETER (MM)',90.,.13)
0133      CALL SYMBOL(-5.5,0.,.1,NOZID,90.,1TEX+12)
0134      CALL SYMBOL(-5.25,0.,.1,'WATER PRESSURE (PSI)',90.,.20)
0135      CALL NUMBER(-5.25,2.25,.1,WATP,90.,-1)
0136      CALL SYMBOL(-5.0,0.,.1,'WIND TUNNEL SPEED (FT/SEC)',90.,.26)
0137      CALL NUMBER(-5.0,2.05,.1,WTS,90.,-1)
0138      CALL SYMBOL(-4.75,0.,.1,'DOWNSTREAM STATION (INCH)',90.,.25)
0139      CALL NUMBER(-4.75,2.75,.1,DOWL,90.,-1)
0140      IF (OPEPLO.GT.0) GO TO 600
0141      650      IF (OPEPLO.NE.0) CALL PLOT(0.,0.,999)
0142      800      CALL EXIT
END
  
```

APPENDIX C
DROPLET DATA

DROPLET DATA FOR NEGATIVE 1

Droplet No.	Diameter (mm)								
1	0.5243418	36	1.180004	71	0.6642479	106	0.2157810	141	0.6872163
2	0.1561709	37	0.1412618	72	0.3766983	107	1.201418	142	0.5862319
3	0.1631151	38	0.2864208	73	1.752381	108	0.4589501	143	2.744425
4	0.2258227	39	0.6317422	74	0.1631151	109	0.3296110	144	0.7907299
5	0.5670060	40	0.1245812	75	0.1697756	110	1.016475	145	1.626387
6	0.1489031	41	0.3395512	76	0.5993233	111	0.1153398	146	0.5728415
7	0.2745637	42	0.5179601	77	0.2157810	112	0.2940600	147	1.310009
8	0.3939605	43	0.6387230	78	0.5591305	113	0.4565282	148	2.814229
9	0.1331829	44	0.8436380	79	0.9661503	114	0.2785721	149	0.2052487
10	0.4685126	45	0.6103209	80	0.6211239	115	0.4211615	150	0.1412618
11	0.5937480	46	0.5766991	81	0.3262303	116	1.182819	151	1.342607
12	0.1883491	47	0.7794333	82	0.1331829	117	1.805354	152	0.4185209
13	0.4613593	48	0.7949249	83	0.7094414	118	0.7460029	153	1.160107
14	0.6524605	49	0.1631151	84	0.2535728	119	0.9865682	154	0.3428006
15	0.2354364	50	0.5571443	85	0.2446727	120	0.8317273	155	1.217004
16	0.1489031	51	0.1883491	86	0.6774681	121	1.021913	156	1.093196
17	0.1245812	52	0.4755583	87	0.2621709	122	0.1331829	157	1.231492
18	0.3707657	53	0.1631151	88	0.1823683	123	0.1412618	158	0.1489031
19	0.1245812	54	0.5222232	89	0.6936390	124	1.678713	159	0.5611097
20	0.4893454	55	0.9832113	90	0.1489031	125	0.4825011	160	0.2535728
21	0.3193615	56	0.3967645	91	0.1489031	126	0.5689578	161	0.2446727
22	0.1697756	57	0.4661403	92	0.2825237	127	0.1153398	162	1.889368
23	0.1489031	58	0.7935290	93	0.5551509	128	0.1761845	163	0.5243418
24	0.1245812	59	0.5093269	94	0.4050601	129	0.2306796	164	1.015383
25	0.1489031	60	0.1489031	95	0.7548665	130	0.4589501	165	0.7949249
26	0.8656892	61	0.1489031	96	0.5591305	131	0.6524605	166	0.2306796
27	0.2663659	62	0.2902655	97	0.2535728	132	0.3123417	167	0.5805310
28	0.7047380	63	0.2825237	98	0.3087720	133	0.2400990	168	1.517058
29	0.1561709	64	0.2902655	99	0.1153398	134	0.1941458	169	0.1823683
30	0.6904351	65	0.4637560	100	0.3228141	135	1.315076	170	0.1631151
31	0.1823683	66	0.3492087	101	0.6121347	136	0.1245812	171	1.431329
32	1.167727	67	1.727532	102	0.1761845	137	0.4732214	172	0.9820831
33	0.1823683	68	0.1561709	103	0.4131892	138	0.3395512	173	1.015383
34	0.1941458	69	1.462741	104	0.6387230	139	0.7264272	174	0.2825237
35	0.4104974	70	0.1561709	105	0.3967645	140	0.4237855	175	0.5974706

DROPLET DATA FOR NEGATIVE 1 (cont'd)

Droplet No.	Diameter (mm)						
176	0.1941458	211	0.3296110	246	0.1823683		
177	0.9684424	212	1.373626	247	1.751115		
178	0.4565282	213	0.3825389	248	0.5805310		
179	0.6507592	214	0.8087506	249	0.1489031		
180	0.4960953	215	0.1153398	250	0.2157810		
181	0.5900019	216	0.6642479	251	0.2704958		
182	0.4708728	217	1.852632	252	0.6575381		
183	0.2258222	218	0.1761845	253	0.1412618		
184	0.3262303	219	0.5264518	254	0.1245812		
185	1.063381	220	0.2825237	255	0.3939605		
186	0.1941458	221	0.5786182	256	0.2902655		
187	1.131075	222	0.2864208	257	0.3647365		
188	0.2579077	223	0.3123417	258	0.4315621		
189	0.1561709	224	0.5430371	259	0.5049549		
190	0.5027546	225	0.1823683	260	0.6103209		
191	0.5786182	226	0.5071455	261	0.1412618		
192	0.6541575	227	0.3296110	262	0.7822727		
193	0.3262303	228	0.3616843	263	1.276578		
194	1.575138	229	0.5591305	264	0.2354364		
195	0.1245812	230	0.1331829	265	0.7031631		
196	0.5571443	231	0.4825011	266	0.8410058		
197	0.2354364	232	0.1941458	267	0.5450747		
198	0.5974706	233	0.2306796				
199	1.077877	234	0.5551509				
200	0.35555012	235	0.3428006				
201	0.2258227	236	0.1412618				
202	0.4467092	237	0.1331829				
203	2.063262	238	0.7233686				
204	0.2785721	239	0.5709030				
205	0.3825389	240	0.2400990				
206	2.363294	241	0.1697756				
207	0.3586060	242	0.2208589				
208	0.4801979	243	0.5264518				
209	1.219733	244	0.2208589				
210	0.4516453	245	0.5974706				

DROPLET DATA FOR NEGATIVE 2

Droplet No.	Diameter (mm)								
1	0.1331829	36	0.8488781	71	0.4392009	106	0.4755583	141	0.3123417
2	0.7533965	37	0.6952354	72	0.3586060	107	1.302370	142	1.726248
3	0.6984173	38	0.6121347	73	0.4847932	108	0.3329574	143	0.9752867
4	0.4516453	39	0.1761845	74	0.1153398	109	0.1561709	144	2.713552
5	0.2864208	40	1.190294	75	0.4938556	110	0.1823683	145	0.4211615
6	0.4847932	41	1.405538	76	0.3395512	111	0.9008328	146	0.6807330
7	0.4801979	42	0.3193615	77	0.2105807	112	1.164875	147	0.1245812
8	0.4392009	43	1.278314	78	0.3523690	113	0.5531504	148	0.2208589
9	0.6456283	44	0.1561709	79	0.5093269	114	0.2354364	149	0.2208589
10	0.2745637	45	0.5114988	80	0.2306796	115	1.724963	150	0.2105907
11	0.1489031	46	0.3123417	81	0.3737437	116	0.8566780	151	1.266114
12	0.7665254	47	0.7294731	82	1.057107	117	1.191225	152	1.673421
13	0.7015847	48	0.7294731	83	0.3737437	118	0.8656892	153	1.363907
14	0.5264518	49	0.7822227	84	0.7294731	119	0.2940600	154	1.805948
15	0.1697756	50	0.8896880	85	0.6456283	120	0.3296110	155	0.1489031
16	0.2785721	51	1.473313	86	0.8462621	121	0.3296110	156	0.7951019
17	0.1883491	52	0.9638526	87	0.5805310	122	0.4613593	157	0.1997744
18	0.2704958	53	0.5049549	88	0.1941458	123	0.3939605	158	0.4237855
19	0.7309912	54	0.8290572	89	0.3296110	124	0.2902655	159	0.3492087
20	0.2491625	55	0.3586660	90	0.5049549	125	0.1331829	160	0.7365127
21	0.1992744	56	1.272314	91	0.2535728	126	0.2052487	161	1.122219
22	0.3939605	57	0.3428006	92	0.2208589	127	0.9546068	162	0.2535728
23	0.2978061	58	0.5179601	93	0.4540953	128	1.173409	163	0.1561709
24	0.2306796	59	1.052904	94	0.5913780	129	0.2579077	164	0.6473432
25	0.5368776	60	1.296398	95	0.5862310	130	0.6575381	165	0.7694125
26	0.1245812	61	0.1245812	96	0.4289875	131	1.224269	166	0.1631151
27	0.1561709	62	1.161062	97	0.3193616	132	0.5551509	167	0.1489031
28	0.1245812	63	0.9592409	98	0.6659143	133	0.1631151	168	0.4211615
29	0.4613593	64	1.346906	99	0.2306796	134	2.012671	169	0.3193615
30	0.8859419	65	1.190294	100	0.6030114	135	0.5436371	170	0.6175439
31	0.4983250	66	0.8169339	101	0.3766983	136	0.2745637	171	0.1331829
32	0.9317273	67	1.261778	102	0.1331829	137	0.9009328	172	0.3596660
33	0.3797965	68	0.2446727	103	0.2621769	138	0.1306298	173	1.092255
34	0.1561709	69	0.4050601	104	0.92531193	139	1.197721	174	0.6282227
35	0.9752867	70	0.4835011	105	0.1761945	140	0.34560104	175	1.071688

DROPLET DATA FOR NEGATIVE 2 (cont'd)

Droplet No.	Diameter (mm)						
174	1.120242						
177	0.225822						
178	0.8644027						
179	0.1245812						
180	0.2052487						
181	1.320964						
182	0.2157810						
183	0.6839823						
184	0.1331829						
185	0.1331829						
186	0.2052487						
187	0.3825389						
188	0.1941458						
189	0.3492087						
190	0.1412618						
191	0.3796298						
192	0.2704958						
193	0.4661403						
194	0.2978061						
195	0.2400990						
196	0.4938556						
197	1.672096						
198	0.2400990						
199	0.1153398						
200	0.3395512						
201	0.5071455						
202	0.4847932						
203	0.3586060						
204	1.110302						
205	0.1883491						
206	0.6352422						
207	0.2579077						

DROPLET DATA FOR NEGATIVE 3

Droplet No.	Diameter (mm)								
1	0.2052487	36	0.4916057	71	0.3854260	106	0.4315621	141	0.4870746
2	0.5709030	37	0.1631151	72	0.1883491	107	0.1631151	142	0.3911363
3	0.1561709	38	0.3882917	73	0.4104974	108	0.2105807	143	1.613871
4	0.7294731	39	0.5158154	74	0.2400990	109	0.9650021	144	0.4392009
5	0.3329574	40	0.2579077	75	0.3158711	110	0.4315621	145	0.2306796
6	0.1245812	41	0.2354364	76	0.1331829	111	0.1697756	146	0.4589501
7	0.3882917	42	0.1561709	77	0.2208589	112	0.1245812	147	0.8114876
8	0.4050601	43	0.5136616	78	0.8087506	113	1.2041833	148	0.2745637
9	0.5071455	44	0.2208589	79	0.3296110	114	1.467281	149	0.2052487
10	0.2446727	45	0.2940600	80	1.197721	115	0.1761845	150	0.3262303
11	0.1153398	46	0.1245812	81	0.2105807	116	0.1331829	151	0.1631151
12	0.1997744	47	0.5264518	82	0.3882917	117	0.6011702	152	0.3051605
13	0.9322907	48	0.1631151	83	0.4050601	118	0.2400990	153	0.1761845
14	1.322641	49	0.2258227	84	0.1823683	119	3.194656	154	0.7094414
15	0.2902655	50	0.9298993	85	0.2491625	120	1.217914	155	0.7125599
16	0.4392009	51	0.1489031	86	0.2258227	121	0.2745637	156	0.4392009
17	0.1245812	52	0.4916057	87	0.4870746	122	0.5862319	157	0.1561709
18	0.1331829	53	0.1697756	88	0.3647365	123	0.2825237	158	0.3939605
19	0.3123417	54	0.2663659	89	0.1997744	124	0.2253227	159	0.5900019
20	0.3015057	55	0.6609015	90	0.1631151	125	0.2157810	160	0.1331829
21	0.6609015	56	0.7851019	91	0.1997744	126	0.3911363	161	0.9405672
22	0.1489031	57	0.7519236	92	0.3362705	127	1.5265529	162	0.1697756
23	0.6524605	58	0.2940600	93	0.7990977	128	0.3523696	163	0.6642479
24	0.2052487	59	1.053956	94	0.2491625	129	1.961342	164	1.213354
25	0.6229062	60	0.4491840	95	0.3677634	130	1.411834	165	0.6592219
26	0.5114988	61	0.7650778	96	0.6888276	131	0.4732214	166	1.418884
27	0.1245812	62	0.3395512	97	1.017565	132	0.4637569	167	0.1331829
28	0.1941458	63	0.4237855	98	0.1697756	133	0.2354364	168	0.6741874
29	0.6524605	64	1.192155	99	0.2105807	134	2.418930	169	0.7851019
30	0.3362705	65	0.3677634	100	0.4131892	135	1.812096	170	0.2491627
31	0.3228141	66	0.2825237	101	0.1412618	136	0.1153398	171	0.1153398
32	0.3796298	67	2.182332	102	2.134566	137	0.1153398	172	0.6968281
33	0.2785721	68	1.173409	103	0.2208589	138	0.4825011	173	0.6234557
34	0.6334946	69	0.2785721	104	1.887607	139	0.1561709	174	0.8449511
35	0.9370274	70	0.3647365	105	0.5571443	140	0.2052487	175	1.965295

DROPLET DATA FOR NEGATIVE 3 (cont'd)

<u>Droplet No.</u>	<u>Diameter (mm)</u>						
176	0.2446727	211	0.7607183	246	0.2157810		
177	0.9695865	212	0.2902655	247	0.5650474		
178	0.1597756	213	0.6439089	248	0.5179601		
179	0.2208589	214	0.9730106	249	0.1245812		
180	0.2663659	215	0.4237855	250	0.7708520		
181	1.068581	216	0.1997744	251	0.5264518		
182	0.7340181	217	0.3262303	252	0.8884411		
183	0.5956123	218	0.4637560	253	0.2306796		
184	0.1245812	219	0.1331829	254	0.3123417		
185	0.5285534	220	0.1697756	255	0.9684424		
186	0.4755583	221	0.2052487	256	0.1997744		
187	0.2621709	222	0.1412619				
188	0.2864208	223	0.7935290				
189	0.1697756	224	0.2745637				
190	0.1331829	225	0.5974706				
191	0.7340181	226	0.3707657				
192	0.8236910	227	0.4708728				
193	0.4131892	228	0.6936390				
194	0.1331829	229	0.1883491				
195	0.3796298	230	0.3677634				
196	0.1245812	231	0.8182897				
197	1.225175	232	0.5862319				
198	0.3586060	233	0.2663659				
199	0.1631151	234	0.6299849				
200	0.1697756	235	0.3586060				
201	0.1153398	236	0.1489031				
202	0.1941458	237	0.9130563				
203	0.1331829	238	0.2258227				
204	0.5805310	239	0.5005447				
205	1.020828	240	0.7031631				
206	1.9681113	241	0.4185209				
207	0.1761845	242	0.5114988				
208	0.1561709	243	0.2621709				
209	1.074787	244	0.9775574				
210	0.1412618	245	0.8410058				

DROPLET DATA FOR NEGATIVE 4

Droplet No.	Diameter (mm)								
1	0.5709030	36	0.9499502	71	0.7636274	106	0.2208589	141	0.6456283
2	0.8707965	37	0.6558500	72	0.3228141	107	0.6524605	142	0.4366695
3	0.3707657	38	2.033495	73	0.2579077	108	1.17269	143	0.2400990
4	0.3766983	39	0.9603959	74	0.1245812	109	0.1331829	144	0.1697756
5	0.5766991	40	0.2354364	75	0.4366695	110	0.1412618	145	0.4211615
6	0.1561709	41	0.7765834	76	0.5071455	111	0.1489031	146	0.4050601
7	0.2978061	42	0.4185209	77	0.3329574	112	0.6103209	147	0.5179601
8	0.1697756	43	0.9166915	78	0.5136616	113	0.4185209	148	0.1561709
9	0.2157810	44	0.3707657	79	1.669442	114	0.8644077	149	0.2105807
10	0.5747736	45	0.5918780	80	0.6317422	115	1.376850	150	0.8032488
11	1.004406	46	1.460465	81	0.3015057	116	0.2446727	151	0.6369849
12	0.2052487	47	0.7694125	82	1.760586	117	0.3737437	152	0.1883491
13	0.4315621	48	0.4778837	83	1.650743	118	0.7141140	153	0.1631151
14	0.3586060	49	0.1761845	84	0.8707965	119	0.8746075	154	0.1631151
15	0.9944228	50	0.5327318	85	1.136941	120	0.6473432	155	0.4211615
16	0.3523690	51	0.3939605	86	0.2785721	121	1.266989		
17	0.2354364	52	0.6246834	87	0.8317273	122	0.5049549		
18	0.9786908	53	0.9057420	88	1.728174	123	0.2940600		
19	0.7851019	54	0.3460194	89	2.441738	124	0.6659148		
20	0.2579077	55	0.4131892	90	0.8004838	125	1.347552		
21	0.3087720	56	0.3616843	91	0.6085018	126	0.5049549		
22	0.3677634	57	0.5005447	92	0.5650474	127	0.2052487		
23	0.1153393	58	0.2157810	93	0.1489031	128	0.3428006		
24	1.345082	59	0.1331829	94	0.1631151	129	0.1245812		
25	0.6725409	60	0.7355269	95	0.5491273	130	0.8370419		
26	0.3329574	61	0.7577981	96	0.1245812	131	0.2258227		
27	1.102235	62	0.4131892	97	0.1997744	132	0.2400990		
28	0.2157810	63	0.2208589	98	0.2258227	133	0.5709030		
29	1.245812	64	0.1631151	99	0.1823603	134	0.8846897		
30	1.881725	65	0.5670060	100	0.1883491	135	0.1153398		
31	0.3911363	66	0.6741873	101	1.226923	136	0.24914625		
32	1.237778	67	0.8983681	102	0.3158711	137	0.6421849		
33	0.1761845	68	0.7415313	103	0.8018675	138	0.3492087		
34	1.422065	69	0.6473432	104	0.4516453	139	0.4613593		
35	0.3995438	70	0.1761845	105	0.5900019	140	0.3051605		

DROPLET DATA FOR NEGATIVE 5

Droplet No.	Diameter (mm)								
1	0.3340937	36	1.156278	71	1.072224	106	0.2446727	141	0.3429067
2	0.2325342	37	2.265579	72	0.3362795	107	0.8223441	142	0.3015057
3	0.1482031	38	0.8771389	73	0.2621709	108	0.5843378	143	0.4613591
4	0.4237855	39	0.8784014	74	1.262607	109	0.3925389	144	0.5591367
5	0.4211613	40	0.1631151	75	0.3296110	110	0.4960953	145	0.4164971
6	0.2535734	41	0.1697754	76	0.1823683	111	0.1489031	146	1.127149
7	0.2978641	42	0.7365254	77	0.1412611	112	0.4755566	147	1.347574
8	0.4825611	43	0.2157814	78	0.4847934	113	0.9106247	148	0.1153374
9	0.2940677	44	0.3939604	79	0.1761844	114	6.326894	149	6.2785794
10	0.1945811	45	1.8817245	80	0.7227951	115	0.4516467	150	0.4366691
11	0.7548641	46	0.4289854	81	1.1884249	116	0.2579077	151	0.1697766
12	0.1761641	47	1.636706	82	1.0273541	117	0.3228141	152	0.5862347
13	0.3169347	48	0.3228141	83	0.6175431	118	1.006611	153	0.3228141
14	0.1922714	49	0.9999814	84	1.9944110	119	0.2864200	154	0.2825247
15	0.1692774	50	1.391263	85	0.8357164	120	1.3549360	155	0.3523690
16	0.5295514	51	0.7325062	86	0.1489031	121	0.1489031	156	0.2306796
17	0.4366604	52	0.1331829	87	0.4211615	122	0.3362795	157	1.028492
18	0.9557674	53	0.3911363	88	3.5481445	123	2.1721442	158	0.1331829
19	0.9843374	54	0.1631151	89	1.033778	124	0.9429231	159	0.2621709
20	0.5179691	55	0.7294731	90	0.1331829	125	1.215490	160	0.4870746
21	0.5243413	56	1.098255	91	0.5611097	126	0.4315621	161	0.2306796
22	0.7679704	57	0.2902655	92	0.2446727	127	0.3555012	162	0.2663659
23	0.1823683	58	0.5409917	93	0.2535729	128	0.5430321	163	0.3555012
24	0.6456283	59	0.2940600	94	0.6558500	129	0.6352421	164	0.8357164
25	0.9382074	60	0.6030114	95	0.6952354	130	0.2208589	165	0.7708520
26	0.5766991	61	0.2306796	96	2.299094	131	0.7794333	166	0.4847932
27	0.7172121	62	0.2354364	97	0.1412616	132	1.495716	167	0.5114988
28	0.1997744	63	0.5993233	98	0.1489031	133	0.2258227	168	0.3466194
29	0.7430248	64	1.044446	99	0.1331829	134	0.5918780	169	0.7694125
30	2.168061	65	0.1331829	100	0.3158711	135	0.1153398	170	0.1153398
31	0.4825011	66	0.2400990	101	0.2208589	136	0.5285534	171	0.1697756
32	1.548162	67	0.7325062	102	0.4801979	137	0.2400990	172	0.2825237
33	1.087094	68	0.3616843	103	0.3737437	138	0.5306467	173	0.5591365
34	1.122219	69	0.6066772	104	0.6369849	139	0.4263935	174	0.2105807
35	1.032705	70	0.2306796	105	0.5491273	140	0.8605515	175	0.1412618
								176	0.6246834
								177	0.4637560
								178	0.3296110
								179	0.9786908

DROPLET DATA FOR NEGATIVE 6

Droplet No.	Diameter (mm)								
1	0.3395512	36	0.4732214	71	0.5200961	106	0.2258227	141	0.8343887
2	0.6299849	37	0.6904351	72	0.4366695	107	0.4185209	142	0.1153398
3	0.2354364	38	0.5388776	73	0.1489031	108	0.2258227	143	0.2258227
4	0.4185209	39	0.4104974	74	0.6524605	109	0.1489031	144	0.7047380
5	0.6439089	40	0.8004838	75	1.357388	110	0.5027546	145	0.8644077
6	0.3523690	41	0.6872163	76	0.1245812	111	0.8087506	146	0.2491625
7	0.4565282	42	0.4685126	77	0.4237855	112	2.016524	147	0.5285534
8	0.1489031	43	0.1331829	78	0.2354364	113	0.2105807	148	0.2208589
9	0.5974766	44	0.7963182	79	0.2704959	114	0.4104974	149	1.5988889
10	0.4341233	45	0.6246834	80	0.6404563	115	0.3015057	150	0.8423229
11	0.3395512	46	0.2400990	81	0.2745637	116	1.681352	151	0.4893454
12	0.5786182	47	0.3586060	82	0.7031631	117	2.049785	152	1.0633881
13	0.1245812	48	1.109303	83	0.6317422	118	0.1153398	153	0.3395512
14	0.4131892	49	0.4613593	84	0.1412619	119	0.5747736	154	0.1823683
15	0.3193615	50	0.3492087	85	0.6968281	120	0.9534448	155	0.1883491
16	0.2208597	51	0.9622018	86	0.6085018	121	0.4104974	156	1.217004
17	0.4158636	52	0.3707657	87	0.8330591	122	0.4613593	157	0.4708728
18	0.4417179	53	0.2978061	88	0.4050601	123	0.2579077	158	0.7489691
19	0.2940600	54	0.2940600	89	0.3939605	124	1.502372	159	2.133007
20	0.6791024	55	0.3586060	90	0.2864208	125	0.4708728	160	1.120242
21	0.1412618	56	0.4477432	91	1.097245	126	0.1412618	161	0.9786908
22	0.1883491	57	0.3555012	92	1.731378	127	0.1153398	162	1.370394
23	0.3228111	58	1.387278	93	2.829158	128	0.3555012	163	0.3329574
24	0.2306796	59	0.2354364	94	0.4467092	129	2.176737	164	0.2864208
25	0.2902655	60	0.9008328	95	0.7607183	130	1.996079	165	0.3193615
26	0.3911363	61	0.6541575	96	0.1823683	131	0.5136616	166	0.5158154
27	0.2306796	62	0.3123417	97	0.3911363	132	0.3967645	167	0.3015057
28	0.6421849	63	0.2902655	98	0.8032489	133	0.4938556	168	1.685304
29	0.3158711	64	0.3677631	99	0.1697756	134	0.3193615	169	0.6692361
30	0.5409917	65	0.9865882	100	0.5881200	135	1.280913	170	0.1331829
31	0.4732214	66	1.689246	101	0.1245812	136	1.041257	171	0.3766983
32	0.4417179	67	0.6030114	102	0.1245812	137	1.163923	172	0.6473432
33	0.9346552	68	0.1331829	103	0.2306786	138	0.4893454	173	0.2052487
34	0.5339386	69	0.1153398	104	0.2446727	139	0.5285534	174	0.1631151
35	0.5179661	70	0.4322009	105	0.9358413	140	0.2978061	175	0.5179601

DROPLET DATA FOR NEGATIVE 6 (cont'd)

Droplet No.	Diameter (mm)						
176	0.1489031						
177	0.4289856						
178	0.6952351						
179	0.1697756						
180	0.4613593						
181	0.4870746						
182	1.1856227						
183	0.4185209						
184	0.2785721						
185	0.4613593						
186	0.6439099						
187	0.5348087						
188	0.2785721						
189	0.2621709						
190	0.4050601						
191	0.6264555						
192	0.8859419						
193	0.2491625						
194	0.8527870						
195	0.1997744						
196	0.1761845						
197	0.1412618						
198	0.6334946						
199	0.6229062						
200	0.3647365						
201	0.3460194						
202	0.1941458						
203	0.3523690						
204	0.6066772						
205	0.5824375						
206	0.3395512						
207	0.1489031						
208	0.5843378						
209	0.3395512						
210	0.1761845						
211	0.1823683						
212	0.3262303						

DROPLET DATA FOR NEGATIVE 7

Droplet No.	Diameter (mm)								
1	0.6558500	36	0.3087720	71	0.6952354	106	0.3087720	141	0.2785721
2	0.1331829	37	1.093255	72	0.2446727	107	0.6541575	142	0.2256261
3	0.4366695	38	0.3677634	73	0.6282227	108	0.2579077	143	0.8846897
4	0.2208589	39	1.165826	74	1.206942	109	1.068581	144	1.250254
5	0.4263935	40	0.1761845	75	0.1245812	110	1.762474	145	0.3262303
6	0.1489031	41	0.3523690	76	0.2785721	111	0.2621709	146	0.5158154
7	0.7607183	42	0.9615495	77	0.5071455	112	0.5027546	147	1.154359
8	0.8475711	43	0.3492087	78	0.3051695	113	0.3051605	148	0.3395512
9	0.2491625	44	0.3616843	79	0.2203589	114	0.5049549	149	0.6968281
10	0.3616843	45	0.2902655	80	0.6459148	115	1.515596	150	0.5158154
11	0.1153393	46	0.3766983	81	0.5306467	116	0.1823683	151	0.5430371
12	0.2940600	47	0.6659148	82	0.3329574	117	0.4467092	152	0.1631151
13	0.8004838	48	0.1245812	83	1.243140	118	0.9672971	153	0.1489031
14	1.097245	49	0.6157461	84	0.1697756	119	0.9921906	154	1.252026
15	0.1245812	50	0.8196434	85	0.1489031	120	0.7751545	155	0.5179601
16	0.1412618	51	0.4776937	86	0.3051605	121	1.159151	156	1.382475
17	0.1631151	52	0.3296116	87	0.1697756	122	0.1245812	157	0.1412616
18	0.1245812	53	0.5471048	88	1.7332298	123	1.106301	158	0.3428601
19	0.2621709	54	0.3262303	89	0.8209949	124	0.2052487	159	0.1457111
20	0.4703728	55	1.220642	90	0.4685126	125	0.1153398	160	0.91163
21	0.5591305	56	0.1245812	91	0.1944958	126	1.739407	161	0.33659
22	0.4916057	57	0.3586060	92	0.4263935	127	0.3228141	162	0.273099
23	0.3329574	58	0.1883491	93	0.3616843	128	2.0438227	163	1.241355
24	0.1153398	59	0.6592219	94	0.4893454	129	1.6695142	164	0.2446727
25	0.3158711	60	0.9592409	95	0.5993233	130	2.414992	165	0.6774691
26	0.1997744	61	0.2105807	96	0.1489031	131	0.9820831	166	0.5368776
27	0.6193365	62	0.8644077	97	0.4685126	132	1.233291	167	0.4315621
28	0.5158154	63	0.2105807	98	0.4077878	133	2.761740	168	0.7000028
29	0.3995488	64	0.6499634	99	0.3037720	134	0.1412618	169	0.5471048
30	0.7836884	65	1.465148	100	0.1761845	135	0.2491625	170	0.7822727
31	0.4077873	66	0.3051604	101	0.2785721	136	0.3051605	171	0.4131872
32	0.4801979	67	0.4565280	102	0.5709030	137	0.2446727	172	1.323479
33	0.4077873	68	0.2056487	103	0.39933681	138	0.4023139	173	0.4366695
34	0.9142697	69	1.270709	104	0.4796170	139	1.986615	174	0.1941458
35	0.2400999	70	0.2946609	105	0.2052469	140	0.4589501	175	0.8142152

DROPLET DATA FOR NEGATIVE 7 (cont'd)

Droplet No.	Diameter (mm)						
176	0.7047380	211	0.1489031				
177	0.2535728	212	0.5049549				
178	1.665453	213	0.7047380				
179	1.950573	214	0.4442205				
180	0.1489031	215	0.2208589				
181	0.326277	216	0.3492087				
182	1.211110	217	0.1631151				
183	0.7047380	218	0.2902655				
184	0.444466	219	0.5591305				
185	1.5295534	220	1.570204				
186	0.8259359	221	0.3193615				
187	0.2535728	222	0.3123417				
188	0.3428906	223	0.3193615				
189	0.1697756	224	0.2258227				
190	0.7218341	225	0.2663650				
191	0.3766987	226	1.280617				
192	0.2704958	227	0.4153398				
193	0.8753741	228	0.3295488				
194	0.8087506	229	1.194941				
195	0.1489031	230	1.175297				
196	1.123207	231	0.4211615				
197	0.4516453	232	0.7000028				
198	0.7460029	233	0.294600				
199	0.2135807	234	0.3737437				
200	0.4325011	235	0.2157810				
201	0.2579077	236	0.2306796				
202	0.8317223	237	0.6856012				
203	0.5348097	238	0.4341233				
204	1.0441116	239	0.2157810				
205	1.144436	240	0.7031631				
206	0.2208589	241	0.6507592				
207	0.5974706	242	0.4392009				
208	0.4263935	243	0.3882917				
209	1.573025						
210	0.4825011						

DROPLET DATA FOR NEGATIVE 8

Droplet No.	Diameter (mm)								
1	0.1331829	36	0.1823683	71	0.5114988	106	0.7504478		
2	0.1708728	37	0.5471048	72	0.8656392	107	0.4847932		
3	0.1489031	38	0.3854260	73	0.7340181	108	1.024081		
4	0.4417179	39	0.7694125	74	0.5049549	109	0.3882917		
5	0.8223441	40	0.2105807	75	0.7722889	110	0.2491625		
6	0.3051605	41	0.2306796	76	0.5611097	111	0.1697756		
7	0.8018675	42	1.240462	77	0.1883491	112	0.1631151		
8	0.3616843	43	0.2704958	78	0.2354364	113	0.1331829		
9	0.4158636	44	0.2621709	79	0.5327318	114	0.1941458		
10	0.3707657	45	0.1331829	80	0.9429221	115	0.2621709		
11	0.3647365	46	0.5005447	81	0.7279517	116	0.1245812		
12	0.1941458	47	0.6139430	82	0.5158154	117	0.6404563		
13	0.3766983	48	0.1412618	83	0.3087720	118	0.3123417		
14	1.212440	49	0.2354364	84	0.5993233	119	0.9854638		
15	0.6011792	50	0.6193365	85	0.9933073	120	0.2663659		
16	0.7780096	51	0.3707657	86	1.601660	121	0.3158711		
17	0.2940600	52	0.6575381	87	0.5747736	122	0.2579077		
18	0.4661403	53	0.2400990	88	0.5471048	123	0.1245812		
19	0.2052487	54	0.1489031	89	0.1561709	124	0.7385352		
20	0.3616813	55	0.5531504	90	0.3825389	125	0.4755583		
21	0.8330561	56	1.055007	91	0.2491625	126	0.3395512		
22	1.519079	57	0.2208389	92	0.3854260	127	0.3296110		
23	0.9157810	58	0.8946584	93	0.4077878	128	0.6558500		
24	0.1631151	59	0.5306467	94	0.2621709				
25	0.2978661	60	0.3228141	95	0.7031631				
26	0.5843379	61	0.2052487	96	0.9499502				
27	0.3193645	62	0.4467092	97	0.2208589				
28	0.7078770	63	0.2446227	98	0.4491840				
29	1.2041037	64	0.6264551	99	0.9534448				
30	0.2621390	65	0.4341037	100	0.2446727				
31	0.2825237	66	0.3847935	101	0.5728415				
32	1.2878148	67	1.195867	102	0.2208589				
33	1.035920	68	1.091166	103	0.1997744				
34	0.4685124	69	1.064423	104	0.2400990				
35	0.8540272	70	0.2258227	105	0.3051605				

DROPLET DATA FOR NEGATIVE 9

Droplet No.	Diameter (mm)						
1	0.3798293	36	0.2940600	71	0.3616843	106	0.6282227
2	0.3128006	37	0.1331829	72	0.1245812	107	0.2400990
3	0.2785721	38	0.5005447	73	0.3460194	108	0.3460194
4	0.4117179	39	0.8032489	74	0.6085018	109	1.058155
5	0.2621709	40	0.8669688	75	0.4417179	110	0.5843378
6	0.2535759	41	0.8475711	76	0.6387230	111	0.3153711
7	0.1153398	42	0.4755583	77	0.1631151	112	0.1941458
8	0.4341235	43	0.3051605	78	0.4392002	113	0.5153154
9	0.1883491	44	0.3123417	79	0.1761845	114	0.3228141
10	0.5285534	45	1.057107	80	0.4801979	115	0.6823594
11	0.1631151	46	0.2052487	81	0.1697756	116	0.8809224
12	0.2400990	47	0.1823683	82	0.3262303	117	0.5389384
13	0.1697256	48	0.6642479	83	0.5993233	118	0.1245812
14	0.3015057	49	1.034850	84	0.3796298	119	1.280913
15	0.2105807	50	0.9695865	85	0.4077878	120	0.2940600
16	0.1489031	51	0.8032488	86	1.086074	121	0.1997744
17	0.5956123	52	1.081983	87	0.1153398	122	0.6936390
18	0.5824375	53	0.4708728	88	0.4755583	123	0.2704958
19	0.5071455	54	0.3616843	89	0.6264555	124	0.7094414
20	0.1153393	55	0.1631151	90	0.9358413	125	0.2785721
21	0.9106247	56	0.7650778	91	0.3395512	126	0.2621709
22	0.6011202	57	0.2579077	92	0.7187562	127	0.5491273
23	0.4870746	58	0.5409917	93	0.3051605	128	0.2052487
24	0.6066772	59	0.1412618	94	0.1245812	129	1.457426
25	0.1153398	60	0.4540933	95	1.110302	130	1.011007
26	0.6139430	61	0.5862319	96	1.254680	131	1.091166
27	0.7977092	62	0.3967645	97	1.123207	132	1.500157
28	0.1153398	63	1.579355	98	0.3796298	133	0.4442205
29	0.2902655	64	0.5027546	99	0.5179601	134	0.1997744
30	0.2745637	65	0.5005447	100	0.9877112	135	0.4565282
31	0.2157910	66	0.1561709	101	0.2825237	136	0.1245812
32	0.5766991	67	0.2535728	102	0.6758296	137	0.1331829
33	0.7063093	68	0.2208589	103	0.7094414	138	1.454380
34	0.9191071	69	0.2704958	104	0.1883491	139	0.8821800
35	0.3939605	70	0.8896880	105	0.9057420	140	0.9057420

DROPLET DATA FOR NEGATIVE 9 (cont'd)

Droplet No.	Diameter (mm)						
Droplet No.	Diameter (mm)						
176	0.3395512	211	0.5158154	246	0.1412618	281	0.5728415
177	0.5306467	212	1.194013	247	0.2400990	282	0.8682466
178	0.6642479	213	0.1697756	248	0.6369849	283	0.1245812
179	0.4077878	214	0.2052487	249	0.2535728	284	0.4825011
180	0.6404563	215	0.1331829	250	0.2785721	285	0.1412618
181	0.1561709	216	0.1245812	251	0.7650778	286	0.6421849
182	0.1489031	217	0.3707657	252	1.108303	287	0.6139430
183	0.4023139	218	0.1245812	253	0.4392009	288	2.068091
184	0.2940600	219	0.9094065	254	0.8060045	289	0.1331829
185	0.6264555	220	0.9227185	255	0.2258227	290	1.057107
186	0.2354364	221	0.3228141	256	0.2306796	291	0.1245812
187	0.4732214	222	0.4289856	257	0.1153398	292	0.4263935
188	0.3087720	223	0.4417179	258	0.2621709	293	0.4211615
189	0.1331829	224	0.1153398	259	0.2354364	294	1.180943
190	0.2157810	225	0.1331829	260	0.4050601	295	0.1997744
191	0.4916057	226	0.1631151	261	0.4661403	296	0.2354364
192	0.2621793	227	0.1245812	262	0.3123417	297	0.2105897
193	0.1883491	228	2.887337	263	0.4341233	298	1.730097
194	0.2208539	229	0.2535728	264	1.131075	299	0.9298995
195	0.1561709	230	1.345082	265	0.6725409	300	0.6030114
196	0.6591395	231	0.2157810	266	0.2400990	301	0.6121347
197	0.1153393	232	0.1697756	267	0.2535728	302	0.1761645
198	0.1245812	233	0.9843382	268	0.7309912	303	0.1331829
199	0.7101112	234	1.605697	269	0.1245812	304	0.2491625
200	0.2794643	235	2.434463	270	1.399243	305	1.067543
201	0.6984173	236	0.1489621	271	0.1823683	306	0.9854539
202	0.2764933	237	0.2745637	272	0.1823683	307	0.3158711
203	0.1941193	238	0.4023437	273	0.2978661	308	0.1331829
204	0.7322173	239	0.2621707	274	0.1153393	309	1.239568
205	0.7141176	240	1.2233364	275	1.281778	310	0.2306796
206	0.3555644	241	1.495715	276	0.3015657	311	0.3492087
207	0.2436727	242	0.1823663	277	0.4613593	312	0.1469031
208	1.4065572	243	0.1823663	278	0.2400990	313	0.5389386
209	0.9826044	244	0.30877595	279	0.6856612	314	0.5571443
210	0.9636044	245	1.0423214	280	0.4732217	315	0.2902655

DROPLET DATA FOR NEGATIVE 10

Droplet No.	Diameter (mm)								
1	1.2666023	16	0.12361519	34	0.42634935	70	0.1153398	141	0.4661463
2	0.9764227	37	0.5709930	72	0.5071455	70	0.7400348	142	0.1561169
3	0.1331829	38	0.2306796	73	0.1489031	69	0.1923683	143	0.2253121
4	0.1331829	39	0.9393883	74	0.6558500	109	1.246138	144	0.3766742
5	0.5937480	40	0.5491273	75	0.3193615	110	1.166141	145	0.2825121
6	0.3051605	41	1.074787	76	0.1245312	111	0.5471145	146	0.3586660
7	0.1883491	42	0.1331829	77	0.3882917	112	1.068664	147	0.2306704
8	0.7202969	43	0.6839820	78	1.052904	113	0.8946539	148	0.3939600
9	0.2978061	44	0.6229062	79	0.8155757	114	0.3087552	149	0.2621169
10	0.2825237	45	0.3296110	80	1.203262	115	0.1941456	150	0.4131392
11	0.8343887	46	0.2354364	81	1.666703	116	0.4164129	151	0.3677634
12	1.4740663	47	0.8527270	82	1.376045	117	0.4540133	152	0.1631151
13	0.5071455	48	1.1543559	83	0.2952487	118	0.5222232	153	0.5095347
14	0.3428005	49	1.0942110	84	0.9287064	119	0.3296110	154	0.6675274
15	0.3123417	50	0.3087720	85	0.3223141	120	0.6807230	155	0.5650474
16	0.7751545	51	0.5200961	86	0.1153398	121	1.601660	156	0.2745637
17	0.6085018	52	0.4565282	87	0.4263935	122	1.324432	157	0.4983250
18	0.2940600	53	0.7233686	88	1.727530	123	0.8462621	158	0.9820831
19	0.7607183	54	1.012103	89	0.7708520	124	0.8958937	159	0.7063693
20	0.5200961	55	0.5306467	90	0.1697756	125	0.3616843	160	0.5368776
21	0.6524605	56	1.093196	91	0.2400990	126	0.6175439	161	0.9499502
22	0.2579077	57	0.2446727	92	0.5611097	127	2.599201	162	0.3523690
23	0.4938554	58	0.4315621	93	0.9713706	128	0.2446727	163	0.1631151
24	0.2052487	59	0.7294731	94	1.055007	129	1.465775	164	0.6299849
25	0.7125599	60	1.226983	95	1.303315	130	0.1153398	165	0.3296110
26	0.3523690	61	1.153398	96	0.5243418	131	0.2621709	166	0.6642479
27	0.5179601	62	0.4263935	97	0.1883491	132	0.9522814	167	0.3939605
28	0.1823683	63	0.1823683	98	0.4417179	133	0.1489031	168	0.5450747
29	0.4685126	64	0.1331829	99	1.127148	134	0.6317422	169	0.3015057
30	0.4442205	65	0.3647365	100	0.1153398	135	1.337624		
31	0.2105807	66	1.449799	101	1.292973	136	0.3087720		
32	0.5306467	67	0.1883491	102	0.4983250	137	0.6121347		
33	0.4960953	68	0.1331829	103	2.009364	138	0.6139430		
34	0.3262303	69	0.3329574	104	1.476320	139	0.2446727		
35	0.7415313	70	1.022998	105	0.2306796	140	0.3123417		

APPENDIX D

DISTRIBUTION LIST

Dr. Frank A. Albini
Northern Forrest Fire Lab
Drawer C
Missoula, MT 59806

Mr. Lou Brown, AWS-120
FAA National Headquarters
800 Independence Avenue, SW.
Washington, DC 20591

Mr. A. Allcock
Department of Industry
Abell House, Room 643
John Islip Street, London
SW14 LN ENGLAND

Mr. Don E. Buse
11B12AB
Phillips Petroleum Company
Bartlesville, OK 74004

Mr. Robert D. Anderson, P.E.
Manager of Engineering
Facet/Quantek, Inc.
P.O. Box 50096
Tulsa, OK 74150

Mr. William A. Callanan
ARCO Chemicals Company
1500 Market Street
Philadelphia, PA 19101

Allied Pilot Association
Equipment Evaluation Comm.
P.O. Box 5524
Arlington, TX 76011

Mr. Ronald Camp
BASF Wyandotte Corporation
1609 Biddle Avenue
Wyandotte, MI 48192

Dr. R. L. Altman
NASA ARC
M.S. 234-1
Moffett Field, CA 94035

Mr. Paul Campbell
244 Green Meadow Way
Palo Alto, CA 94306

Dr. S. J. Armour
Defense Research Establishment
Suffield
Ralston, Alberta
CANADA, T0J 2N0

Mr. Clifford D. Cannon
Transamerica Delaval, Inc.
Wiggins Connectors Division
5000 Triggs Street
Los Angeles, CA 90022

Mr. Robert Armstrong
B-8414 MS-9W61
Boeing Airplane Company
P.O. Box 3707
Seattle, WA 98124

Mr. George A. Cantley
Lear Siegler, Inc.
241 South Abbe Road
P.O. Box 4014
Elyria, OH 44036

Mr. Steven L. Baxter
Conoco, Inc.
Chemicals Research Division
P.O. Box 1267
Ponca City, OK 74601

Captain Ralph Cantrell
University of Bridgeport
U.S. Army ROTC Department
Bridgeport, CT 06601

Dr. D. E. Boswell
Quaker Chemical Corporation
Elm Street
Conshohocken, PA 19428

Dr. Homer W. Carhart
Naval Research Lab
Code 6180
Washington, DC 20375

Mr. Michael Cass
Sundstrand Corporation
4747 Harrison Avenue
Rockford, IL 61101

Mr. B. G. Corman
Exxon Research and Engineering
P.O. Box 4255
Baytown, TX 77520

Dr. Young I. Cho, Ph.D.
Drexel University
College of Engineering
Philadelphia, PA 19104

Mr. Dick Coykendall
United Airlines
San Francisco International
Airport
San Francisco, CA 94128

Mr. Arthur V. Churchill
AFWAL/POSH
Wright Patterson Air Force Base
Ohio 45433

Mr. Gerald A. Cundiff
General Electric Company
3 Penn Center Plaza
Philadelphia, PA 19102

Mr. J. C. Clerc
Chevron Research Company
P.O. Box 1627
Richmond, CA 94802-0627

Mr. Rick DeMeis
126 Powers Street
Needham, MA 02192

Mr. George A. Coffinberry
General Electric Company
1 Neumann Way
Mail Drop E-186
Cincinnati, OH 45215

Mr. Terence Dixon
Boeing Aerospace Corporation
P.O. Box 3999
M/S 8J-93
Seattle, WA 98124

Mr. Fred W. Cole
Filter Products Division
Facet Enterprises, Inc.
8439 Triad Drive
Greensboro, NC 27409

Mr. Thomas F. Donohue
General Electric Company
1 Neumann Way, Mail Drop H-44
P.O. Box 156301
Cincinnati, OH 45215-6301

Mr. J. Donald Collier
Air Transport Association
of America
1709 New York Avenue, NW.
Washington, DC 20006

Mr. William G. Dukek
11 Ridge Road
Summit, NJ 07901

Captain Ralph Combariati
Port Authority of NY and NJ
JFK International Airport
Jamaica, NY 11430

Mr. David W. Eggerding
AMOCO Chemicals Corporation
Research and Development
P.O. Box 400
Naperville, IL 60540

Mr. Edward Conklin
Sikorsky Aircraft
North Main Street
Stratford, CT 06602

Dr. Thor Eklund, ACT-350
DOT/FAA Technical Center
Atlantic City Airport, NJ 08405

Mr. John H. Enders
Flight Safety Foundation
5510 Columbia Pike
Arlington, VA 22204

Dr. Allen E. Fuhs
Department of Aeronautics
Naval Post Graduate School
Monterey, CA 93940

Mr. John T. Eschbaugh
Air Maze Incom International
25000 Miles Road
Cleveland, OH 44198

Dr. Gerald G. Fuller
Chemical Engineering
Stanford University
Stanford, CA 94305

Mr. Anthony Fiorentino
Pratt and Whitney Aircraft
EB264
400 Main Street
East Hartford, CT 06108

Y. Funatsu
All Nippon Airways
1-6-6, Tokyo International Airport
Ohta-KU, Tokyo 144
JAPAN

F. Firth
Lucas Aerospace
Vannonstrand Avenue
Englewood, NJ 07632

Henry A. Gill
Lockheed California Company
Building 88, B-6
P.O. Box 551
Burbank, CA 91520

Mr. Kent Fisher
Lockheed California Company
Department 70-30, Building 90
P.O. Box 551
Burbank, CA 91520

Mr. David J. Goldsmith
Eastern Airlines
Miami International Airport
Miami, FL 33148

Mr. David H. Fishman
Technical Planning and Development
United Technologies Inmont
1255 Broad Street
Clifton, NJ 07015

Mr. Stanley Gray
Mechanical Technology Inc.
968 Albany Shaker Road
Latham, NY 12110

Mr. Ray Fitzpatrick
South African Airways
329 Van Riebeeck Road
Glenn Austin Halfway House, 1685
REPUBLIC OF SOUTH AFRICA

Mr. Ray J. Grill
TRW
1766 Sunset Drive
Richmond Heights, OH 44124

Dr. Kendall Foley
Hercules Inc.
Research Center
Wilmington, DE 19899

G. Haigh
Air Canada
Air Canada Base, Montreal
International Airport
Quebec, CANADA H4Y 1 C2

Mr. Robert Friedman
NASA Lewis Research Center
M/S 6-9
21000 Brookpark Road
Cleveland, OH 44135

Lit S. Han
Ohio State University
206 W. 18th Avenue
Columbus, OH 43210

M. Hardy
United Airlines
SFOEG, MOC
San Francisco International Airport
California 94128

Major Hudson
Air Force Inspection and Safety
SEDM
Norton Air Force Base, CA 92499

Cyrus P. Henry
E. I. Dupont De Nemours
and Company
Petroleum Lab
Wilmington, DE 19898

Mr. Stephen L. Imbrogno
Pratt and Whitney Aircraft Group
Government Products Division
M/S 711-52
West Palm Beach, FL 33402

R. Hileman
Texaco, Inc.
Box 509
Beacon, NY 12508

Dr. Wolfgang Immel
BASF Aktiengesellschaft
Technologie und Produktionsplanung
6700 Ludwigshafen
WEST GERMANY

W. Hock
Grumman Aerospace Corporation
B 14 035
111 Stewart Avenue
Bethpage, NJ 11714

M. C. Ingham
Chevron Research Company
P.O. Box 1627
Richmond, CA 94802-0627

Arthur Hoffman
American Cyanimid
1937 West Main Street
Stamford, CT 06904

G. Jahrstorfer
Chandler Evans, Inc.
Charter Oak Boulevard
West Hartford, CT 06110-0651

LCDR William Holland
Department of the Navy
NAIR 518
Naval Air Systems Command
Washington, DC 20361

Mr. J. P. Jamieson
National Gas Turbine Establishment
Pyestock, Farnborough
Hants GU14 0LS
ENGLAND

Robert L. Hoover
Box 10850 Cave Creek Stage
Phoenix, AZ 85020

Mr. Eric Jevons
Chandler Evans, Inc.
Charter Oak Boulevard
Box 10651
West Hartford, CT 06110-0651

Mr. Thomas G. Horeff
Federal Aviation Administration
AEU-101
c/o American Embassy
APO New York 09667-1011

Mr. Stanley Jones
Pan American World Airways
JFK International Airport
New York, NY 11420

Mr. Gary L. Norton
Chemical Research Division
Conoco, Inc.
P.O. Box 1267
Ponca City, OK 74603

R. Kassinger
Exxon International Company
Commercial Department
200 Park Avenue
Florham, NJ 07932

Dr. C. W. Kauffman
The University of Michigan
Gas Dynamics Laboratories
Aerospace Engineering Building
Ann Arbor, MI 48109

Mr. Perry Kirklin
Mobil Research and Development
Corporation
Billingsport Road
Paulsboro, NJ 08066

Mr. R. Kirsch, AWS-120
FAA National Headquarters
800 Independence Avenue, SW.
Washington, DC 20591

Mr. John Kirzovensky
Naval Air Propulsion Center
Code PE71
1440 Parkway Avenue
Trenton, NJ 08628

Mr. W. Peter Kochis
FAA Safety Programs
Division, ASF-300
800 Independence Avenue, SW.
Washington, DC 20591

Mr. Rob Koller
Rohm and Haas
727 Norristown Road
Spring House, PA 19477

Mr. Robert J. Kostelnik
ARCO Chemical Company
3801 West Chester Pike
Newtown Square, PA 19073

Mr. J. I. Knepper
Petrolite Corporation
369 Marshall Avenue
St. Louis, MO 63119

Dr. John Krynnitsky
Fuels and Petroleum Products
4904 Cumberland Avenue
Chevy Chase, MD 20015

Dr. Karl Laden
Carter-Wallace, Inc.
Half Acre Road
Cranbury, NJ 08512

Mr. Thomas P. Lally, Jr.
Senior Marketing Specialist
Aircraft Porous Media, Inc.
Pinellas Park, FL 33565

Dr. R. Landel
Jet Propulsion Lab
4800 Oak Grove Drive
Pasadena, CA 91103

R. Laurens
Rolls-Royce, Inc.
1895 Phoenix Boulevard
Atlanta, GA 30349

Mr. Richard J. Linn
American Airlines
MD 4H14
P.O. Box 61616
Dallas/Fort Worth Airport, TX 75261

P. Longjohn
Clagon Corporation
P.O. Box 1346
Pittsburgh, PA 15230

Mr. Richard R. Lyman
Lear Siegler, Inc.
Energy Products Division
2040 East Dyer Road
Santa Ana, CA 92702

Dr. Richard Mannheimer
Southwest Research Institute
8500 Culebra Road
San Antonio, TX 78284

Captain A. S. Mattox, Jr.
Allied Pilots Association
12723 Brewster Circle
Woodbridge, VA 22191

Mr. James McAbee
ICI Americas, Inc.
Specialty Chemicals Division
Wilmington, DE 19897

Mr. Warren D. Niederhauser
Rohm and Haas Company
727 Norristown Road
Spring House, PA 19477

Mr. Charles McGuire
Department of Transportation
400 7th Street, SW. (P-5)
Washington, DC 20590

J. J. O'Donnell
Airline Pilots Association
1625 Massachusetts Avenue, NW.
Washington, DC 20036

M. L. McMillan
G.M. Research
Fuels and Lubricants Department
Warren, MI 48090

Dean Oliva
Lockheed
Department 7475/Building 229A
P.O. Box 551, Plant 2
Burbank, CA 91520

Mr. Peter Meiklem
British Embassy
3100 Massachusetts Avenue, NW
Washington, DC 20008

Dr. Robert C. Oliver
Institute for Defense Analyses
1801 North Bauregard Street
Alexandria, VA 22311

Mr. G. Chris Meldrum
Texaco Company
P.O. Box 430
Bellaire, TX 77401

Mr. James H. O'Mara
Rohm and Haas
727 Norristown Road
Spring House, PA 19477

Dr. Robert E. Miller
c/o Dr. S. P. Wilford
Royal Aircraft Establishment
Farnborough, Hants
GU146TD, ENGLAND

Mr. George Opdyke
AVCO Lycoming Division
550 South Main Street
Stratford, CT 06497

Mr. Robert J. Moore
Shell Chemical Company
Box 2463
Houston, TX 77001

Dr. Robert H. Page
Texas A&M University
College of Engineering
College Station, TX 77884

Mr. Peter D. Moss
American Hoechst Corporation
Route 206 North
Somerville, NJ 08876

Chris Papastrat
CEE Electronics, Inc.
8875 Midnight Pass Road
Sarasota, FL 33581

Mr. David Nesterok, ACT-2P
DOT/FAA Technical Center
Atlantic City Airport, NJ 08405

Mr. Roy E. Pardue
Lockheed/Georgia Company
86 South Cobb Drive
Marietta, GA 30063

Mr. Sam Paton
El Paso Products
P.O. Box 3986
Odessa, TX 79760

Mr. Tom Peacock
Douglas Aircraft Company
3855 Lakewood Boulevard
Longbeach, CA 90846

R. D. Pharby
Petro Canada
Sheridan Park
Mississauga, Ontario
CANADA, L5K1A8

Mr. John Pullekins
Air Products and Chemicals
Industrial Chemical Division
P.O. Box 538
Allentown, PA 18105

Dr. Andy Powell
Saudia - CC 836
P.O. Box #167
Jeddah
SAUDI ARABIA

Mr. Horst Rademacher
68 Myrtle Street
Boston, MA 02114

Mr. William Radenbaugh
General Electric Company
Manager, Operational Planning
1000 Western Avenue
Lynn, MA 01910

C. C. Randall, P.E.
Lockheed Georgia Company
D72-47 Zone 418
Marietta, GA 30063

Mr. Richard W. Reiter
National Starch and Chemical
Box 6500
10 Finderne Avenue
Bridgewater, NJ 08807

M. Ruppen
Pratt and Whitney Aircraft
Government Products Division
P.O. Box 2691
West Palm Beach, FL 33402

Mr. Charles Rivers
ICI Americas, Inc.
Wilmington, DE 19897

Mr. Russell Rogers
Aeroquip Corporation
Corporate Engineering
Jackson, MI 49203

J. Romans
Hughes Association, Inc.
9111 Louis Avenue
Silver Spring, MD 20910

E. T. Roockey
Northrop Corporation
Aircraft Division
One Northrop Avenue
Hawthorne, CA 90250

Dr. V. Sarohia
Jet Propulsion Lab
M/S 125-214
4800 Oak Grove Drive
Pasadena, CA 91109

Mr. George Savins
Mobil Oil Research and
Development
P.O. Box 819047
Dallas, TX 75381

Dr. Barry Scallet
Anheuser-Busch Corporation
Central Research Inc.
P.O. Box 11841
Clayton, MO 63105

Mr. Forrest W. Schaekel
U.S. Army MERADCOM
Fort Belvoir, VA 22060-5606

Mr. Barry Scott, ADL-31
P.O. Box 25
NASA Ames Research Center
Moffett Field, CA 94035

Dr. Warren C. Strahle
Georgia Institute of Technology
School of Aerospace Engineering
Atlanta, GA 30332

Professor Valentinas Sernas
Rutgers University
College of Engineering
P.O. Box 909
Piscataway, NJ 08854

Mr. Peter A. Stranges
1420 16th Street, NW.
Washington, DC 20006

Mr. Subhash Shah
Allied Chemical
Syracuse Research Lab
P.O. Box 6
Salisbury, NY 13209

Mr. Kurt H. Strauss
Consultant, Aviation Fuels
116 Hooker Avenue
Poughkeepsie, NY 12601

Dr. Hakam Singh, Ph.D.
Product Chemical and Research
Corporation
2920 Empire Avenue
Burbank, CA 91504

Mr. Dick Stutz
Sikorsky Aircraft
Engineering Department
Stratford, CT 06602

Ms. Dana Smith
ARCO Chemical Company
1500 Market Street
32nd Floor
Philadelphia, PA 19101

Mr. A. F. Taylor
Cranfield Institute of Technology
Cranfield, Bedford, MK 43 0AL
ENGLAND

Mr. H. Daniel Smith
Manager, Research and Development
Engineered Fabrics Division
Goodyear Aerospace Corporation
Akron, OH 44315

Dr. W. F. Taylor
Exxon Research and Engineering Company
Products Research Division
P.O. Box 51
Linden, NJ 07036

S. Sokolsky
Aerospace Corporation
P.O. Box 91957
Los Angeles, CA 90009

Dr. James Teng, Ph.D.
Anheuser-Busch Corporation
1101 Wyoming Street
St. Louis, MO 63118

Mr. Leo Stampler
Gull Airborne Instruments, Inc.
395 Oser Avenue
Smithtowne, NY

Mr. Joseph Thibodeau
Goodyear Aerospace Corporation
1210 Massillon Road
Akron, OH 44315

Mr. Barry Stewart
Olin Chemicals
Brandenburg, KY 40108

Mr. Richard G. Thrush
Lear Siegler, Inc.
241 South Abbe Road
P.O. Box 4014
Elyria, OH 44036

Mr. Dick Tobiason
Air Transport Association
1709 New York Avenue, NW.
Washington, DC 20006

Dr. F. F. Tolle
Boeing Military Airplane Company
P.O. Box 3707
M/S 4152
Seattle, WA 98124

Mr. R. Hugh Trask
Southland Corporation
849 Coast Boulevard
LaJolla, CA 93034

M. Trimble
Delta Airlines
DEAT 568
Atlanta International Airport
Atlanta, GA 30320

Mr. T. Ted Tsue
Boeing Aerospace Company
P.O. Box 3999
M/S 45-07
Seattle, WA 98124

Trans World Airlines, Inc.
Kansas City International Airport
2-280
P.O. Box 20126
Kansas City, MO 64195

Mr. Robert Umschied
M.S.E.-6
9709 East Central
Wichita, KS 19328

Mr. Ed Versaw
Lockheed/California Company
P.O. Box 551
Burbank, CA 91520

J. F. Vitkuske
Dow Chemical Company
1702 Building
Midland, MI 48640

Mr. Fred Waite
Imperial Chemical Industries PLC
Paints Division
Mexham Road, Slough SL2 5DS
ENGLAND

Dr. G. J. Walter
Sherwin-Williams Company
501 Murray Road
Cincinnati, OH 45217

H. Weinberg
Exxon Research and
Engineering Company
P.O. Box 45
Linden, NJ 07036

Mr. Paul Weitz
Simmonds Precision Instruments
Panton Road
Vergennes, VT 05491

Mr. John White
National Transportation
Safety Board
800 Independence Avenue, SW.
Washington, DC 20594

Mr. Richard White
Denry White, Inc.
P.O. Box 30088
Cleveland, OH 44130

Dr. S. P. Wilford
Royal Aircraft Establishment
Farnborough, Hants
GU146TD
ENGLAND

R. P. Williams
Phillips Petroleum
107 Catalyst Lab
Bartlesville, OK 74004

R. E. Zalesky
Lockheed California Company
P.O. Box 551
Burbank, CA 91520

Civil Aviation Authority (5)
Aviation House
129 Kingsway
London WC2B 6NN England

DOT-FAA AEU-500 (5)
American Embassy
APO New York, NY 09667

Embassy of Australia (1)
Civil Air Attache
1601 Mass. Ave. NW
Washington, DC 20036

University of California (1)
Service Dept Institute of
Transportation Standard Lib
412 McLaughlin Hall
Berkeley, CA 94720

Scientific & Tech. Info FAC (1)
ATTN: NASA Rep.
P.O. Box 8757 BWI Airport
Baltimore, MD 21240

British Embassy (1)
Civil Air Attache ATS
3100 Mass Ave. NW
Washington, DC 20008

Northwestern University (1)
Trisnet Repository
Transportation Center Library
Evanston, ILL 60201

Director DuCentre Exp DE LA (1)
Navigation Aerineene
9141 Orly, France

ANE-40	(2)	ACT-624	(2)	ASW-53B	(2)
ASW-52C4	(2)	AAL-62	(2)	AAC-44.4	(2)
APM-13 Nigro	(2)	M-493.2 Bldg. 10A	(5)	ACE-66	(2)
AEA-66.1	(3)	APM-1	(1)	ADL-1	(1)
ADL-32 North	(1)	APA-300	(1)	ALG-300	(1)
AES-3	(1)	AGL-60	(2)	ACT-8	(1)
ANM-60	(2)				

FAA, Chief, Civil Aviation Assistance Group (1)
Madrid, Spain
c/o American Embassy
APO-New York 09285-0001

Al Astorga (1)
Federal Aviation
Administration (CAAG)
American Embassy, Box 38
APO-New York 09285-0001

Dick Tobiason (1)
ATA of America
1709 New York Avenue, NW
Washington, DC 20006

Burton Chesterfield, DMA-603 (1)
DOT Transportation Safety Inst.
6500 South McArthur Blvd.
Oklahoma City, OK 73125

FAA Anchorage ACO
701 C Street, Box 14
Anchorage, Alaska 99513

FAA Fort Worth ACO
P.O. Box 1689
Fort Worth, TX 76101

FAA Atlanta ACO
1075 Inner Loop Road
College Park, Georgia 30337

FAA Long Beach ACO
4344 Donald Douglas Drive
Long Beach, CA 90808

FAA Boston ACO
12 New England Executive PArk
Burlington, Mass. 01803

FAA Los Angeles ACO
P.O. Box 92007, Worldway Postal Center
Hawthorne, CA 90009

FAA Brussels ACO
Z American Embassy, APO,
New York, NY 09667

FAA New York ACO
181 So. Frankline Ave., Room 202
Valley Stream, NY 11581

FAA Chicago ACO
2300 E. Devon, Room.232
Des Plains, Illinois 6008

FAA Seattle ACO
17900 Pacific Highway South, C-68966
Seattle, Washington 98168

FAA Denver
10455 East 25th Ave., Suite 307
Aurora, Colorado 98168

FAA Wichita ACO
Mid Continent Airport, Room 100 FAA Bldg.
1891 Airport Road
Wichita, KA 67209

Frank Taylor
3542 Church Road
Ellicott City, MD 21043

E N D

4-87

DTIC